The Way to Fusion Energy

Passive spectroscopy working group

Robin Barnsley

Queen's University Belfast, EFDA/JET, ITER International Team, Cadarache, France.

Fast radiation-hard energy-resolving imaging detectors

ITER x-ray spectrometer array

ITER x-ray camera

γ-Ray Monitoring of Transient Alpha-Particle Losses

V.Kiptily, UKAEA Culham

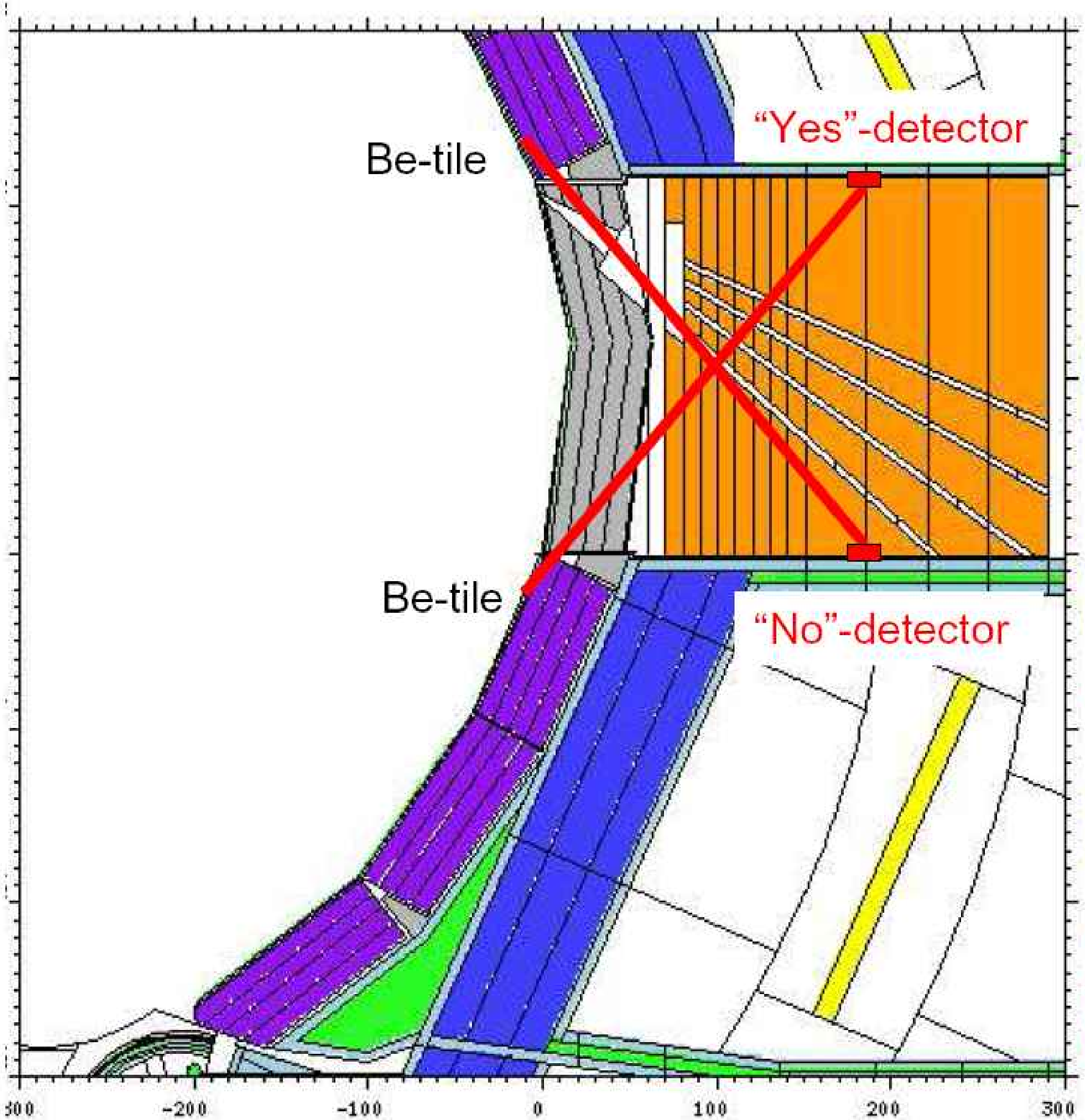

Differential γ-diagnostic system:

4.4-MeV gammas from the ^{9}**Be+α** reaction are measured with **"Yes"**- and **"No"**-detectors through the neutron attenuators.

Lost alpha flux (**E>1.5 MeV**) is derived from the differential signal (**"Yes"-"No"**). Calibration procedure is needed.

Gammas produced by **confined alphas** cannot be seen by these detectors. **Neutron** flux is relatively low.

Thick *Be*-target gamma-yield :

3E-06 γ / α @ 3.5 MeV (Ioffe's exp. data)
2E-05 γ / α @ 5 MeV

10-kHz γ-rate (4.4-MeV) in the compact detector is expected @ 2 MW/m^2 load and the 100-cm^2 viewing area.

High energy physics requires radiation-hard detectors

SLHC core neutron fluence >10^16/cm^2 over 10 yrs

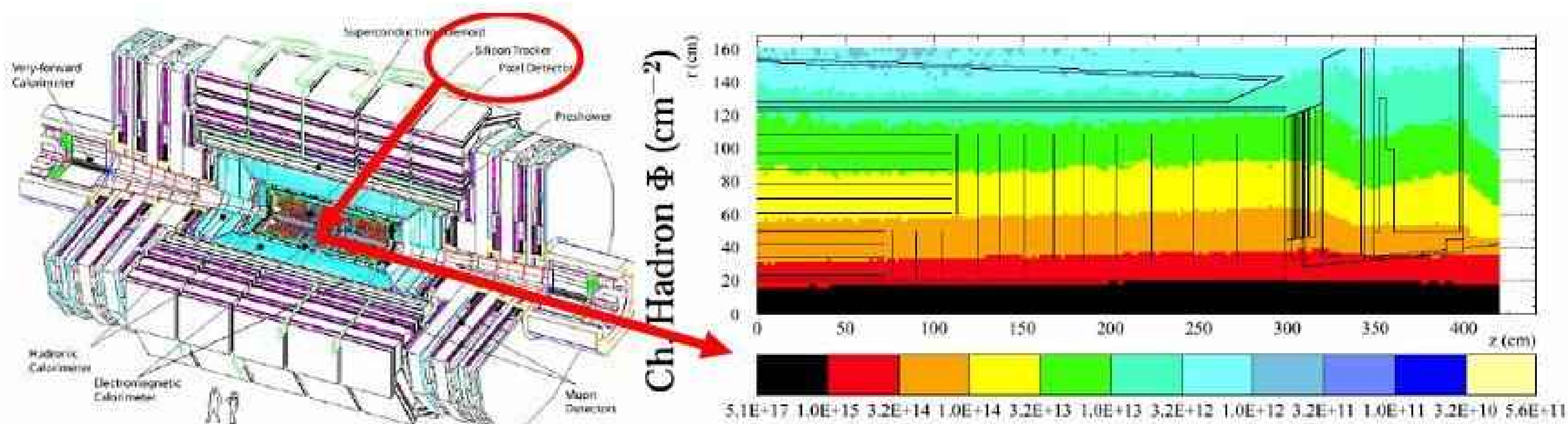

Compact Muon Solenoid M. Hutinen: "Radiation issues for Super-LHC", SLHC Electronics Workshop, 26/2/04, CERN

- **Integrated Luminosity** (radiation damage) dictates the detector **technology**
- **Instantaneous rate** (particle flux) dictates the detector **granularity**

R (cm)	Φ (p/cm²)	Technology
>50	10^{14}	Present p-in-n (or n-in-p)
20-50	10^{15}	Present n-in-n (or n-in-p)
<20	10^{16}	RD needed

RD50 - Radiation hard semiconductor devices for very high luminosity colliders

RD50 **Scientific Organization of RD50**

Development of Radiation Hard Semiconductor Devices for High Luminosity Colliders

Co-Spokespersons

Mara Bruzzi and *Michael Moll*

INFN and University of Florence — CERN PH-DT2

Defect / Material Characterization	Defect Engineering	New Materials	Pad Detector Characterization	New Structures	Full Detector Systems
Bengt Svensson (Oslo University)	*Eckhart Fretwurst* (Hamburg University)	*Elena Verbitskaya* (Ioffe, St.Petersburg)	*Gregor Kramberger* (Ljubljana)	*Richard Bates* (Glasgow University)	*Gianluigi Casse* (Liverpool University)
Characterization of microscopic properties of standard-, defect engineered and new materials pre- and post-irradiation	Development and testing of defect engineered silicon: - Epitaxial Silicon - High res. CZ, MCZ - Other impurities H, N, Ge, … - Thermal donors - Pre-irradiation	Development of new materials with promising radiation hard properties: - bulk, epitaxial SiC - GaN - other materials	• Test structure characterization IV, CV, CCE • NIEL • Device modeling • Operational conditions • Common irradiations • Standardisation of macroscopic measurements (A.Chilingarov)	• 3D detectors • Thin detectors • Cost effective solutions • 3D (M.Rahman) • Semi 3D (Z.Li) • Thinned detectors (M.Boscardin)	• LHC-like tests • Links to HEP • Links to R&D of electronics • Comparison: pad-mini-full detectors • Comparison of detectors made by different producers
• DLTS Calibration (B.Svensson)	• Oxygen Dimer (M.Moll)	• SiC (I.Pintilie) • GaN (J.Vaitkus)			

CERN contact: Michael Moll

Michael Moll – December 05 -

ENERGY-RESOLVED FAST 2-D X-RAY IMAGING

D Pacella ENEA – Frascati , Italy. APS – HTPD , 19-22 April 2004 , San Diego, CA, USA

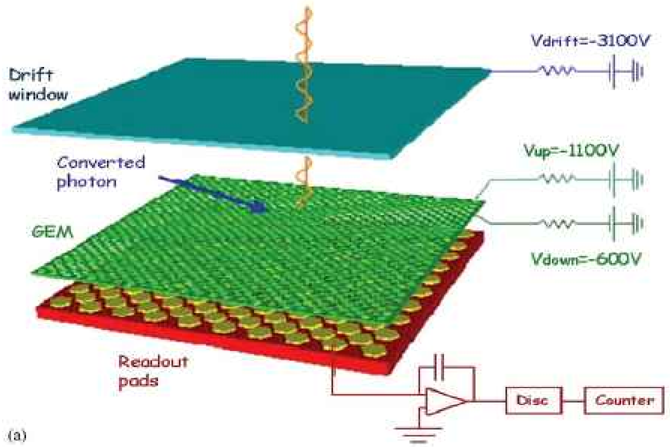

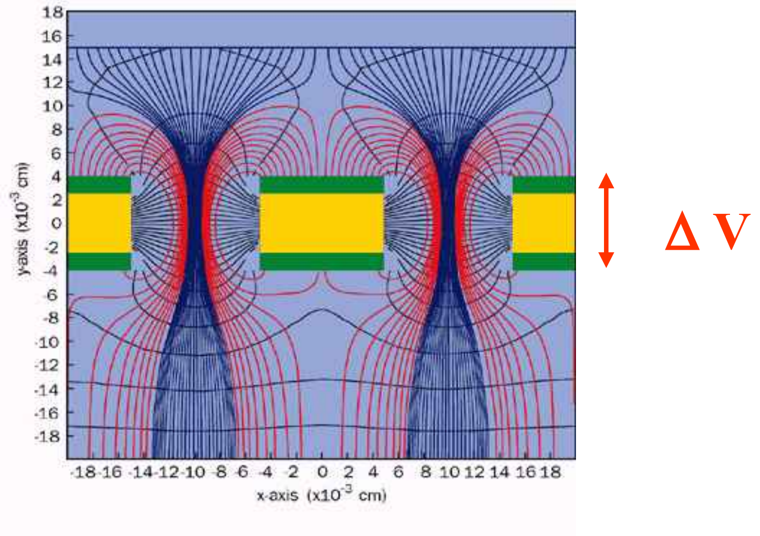

Prototype GEM detector. PIXCS-128 128 pixels

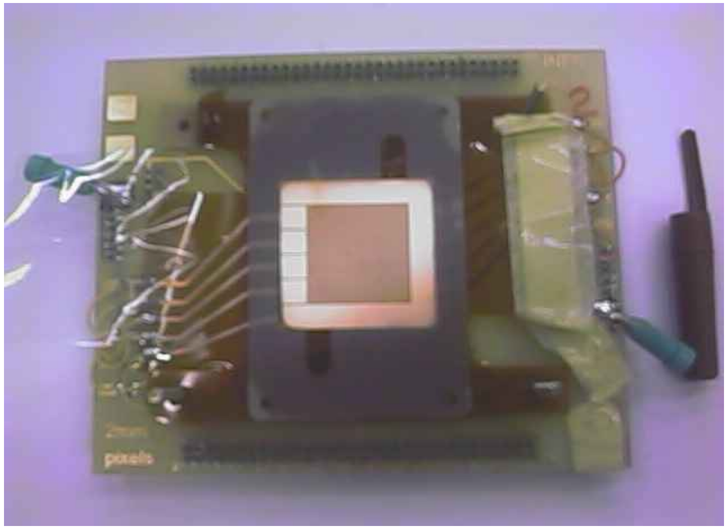

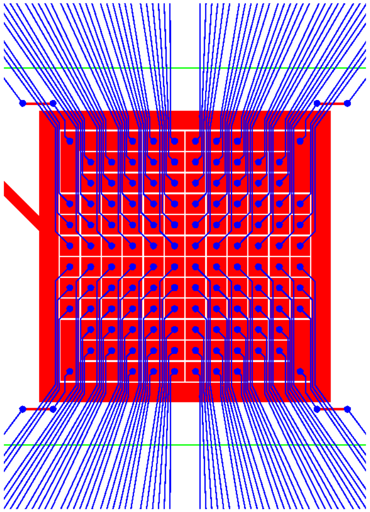

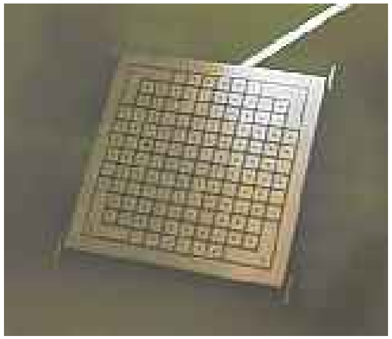

Energy resolution on each pixel in a wide energy range
Independent window analyzer on each pixel, capable of > 10^6 count/s

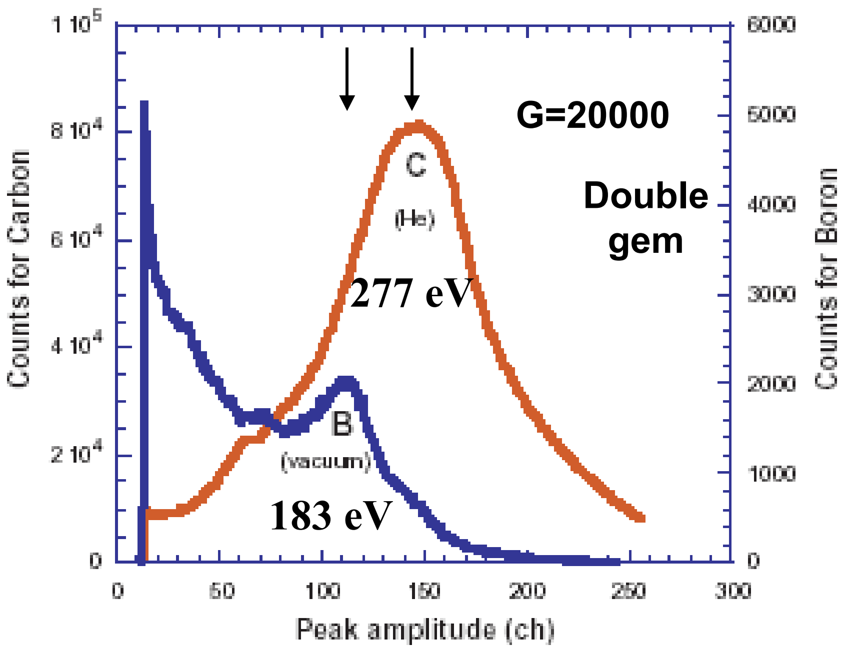

Fig. 4. Spectrum of carbon (277eV, right axis) with double GEM and He between source and detector. Spectrum of boron (183 eV, left axis), with double GEM and vacuum between source and detector.

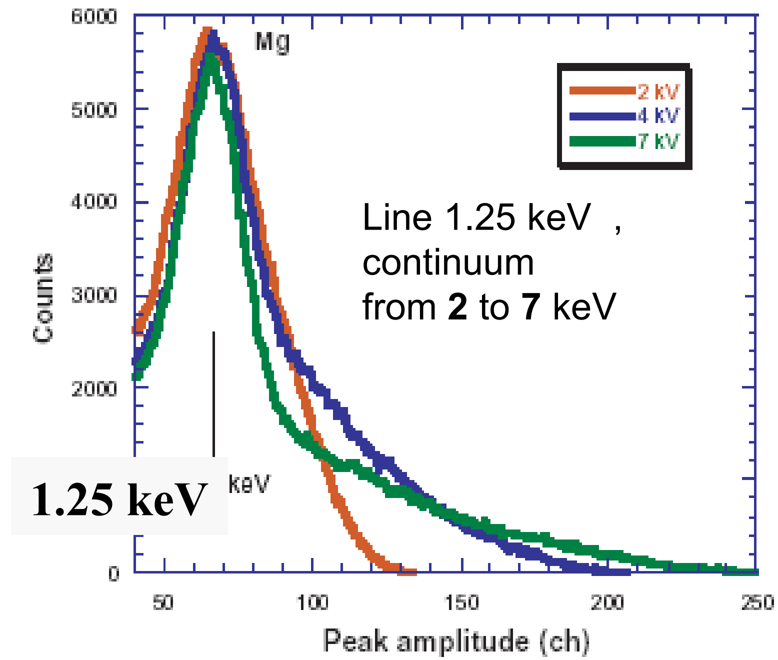

Fig. 5. Spectra of Mg (1.25keV) with different Voltages for the anode of the X-ray source: 2.5kV (red), 4kV (blue), 7kV (green). Spectra are normalized to the peak emission of the K feature.

Steerable, "zoomable" x-ray pin-hole camera with tangential view
Fast spectroscopic imaging is valuable to study Te(r) and cross-field transport

Tangential views of NSTX plasma (Madison, Wisconsin)

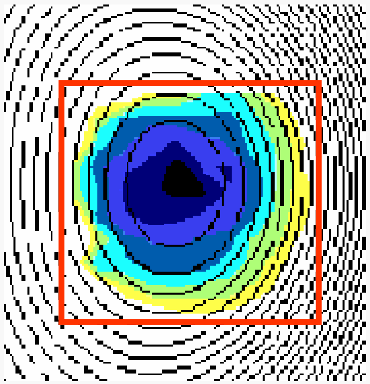
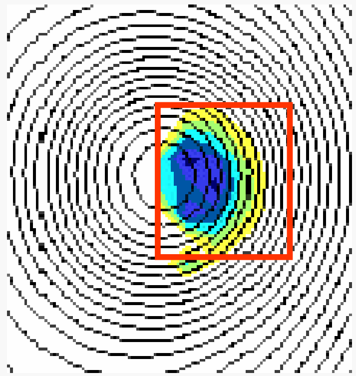
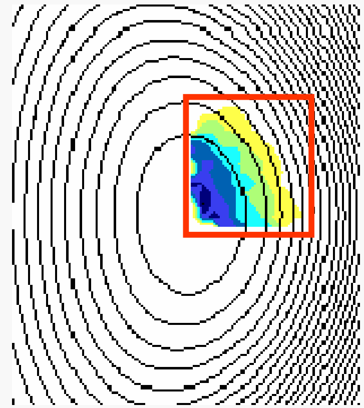
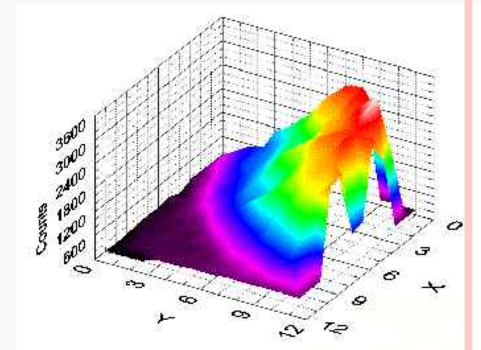

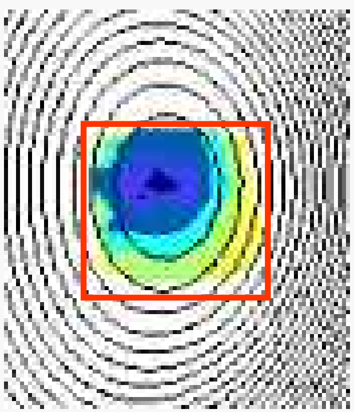
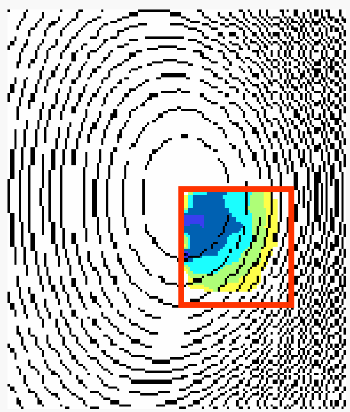
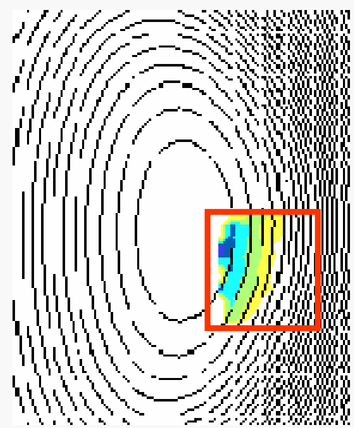
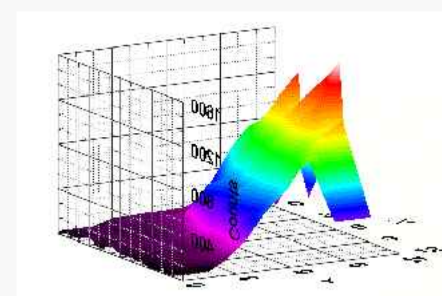

Application of PILATUS II Detector Modules for High Resolution X-Ray Imaging Crystal Spectrometers on the Alcator C-Mod Tokamak

M. L. Bitter [1], Ch. Broennimann [2], E. F. Eikenberry [2], K. W. Hill [1],
A. Ince-Cushman [3], S. G. Lee [4], J. E. Rice [3], S. Scott [1].

[1] *PPPL, Princeton University, Princeton, NJ, USA*
[2] *SLS, Paul Scherrer Institut, Villingen, Switzerland*
[3] *PSFC, Massachussetts Institute of Technology, Cambridge, MA, USA*
[4] *NFRC, Korea Basic Science Institute, Daejeon, Korea*

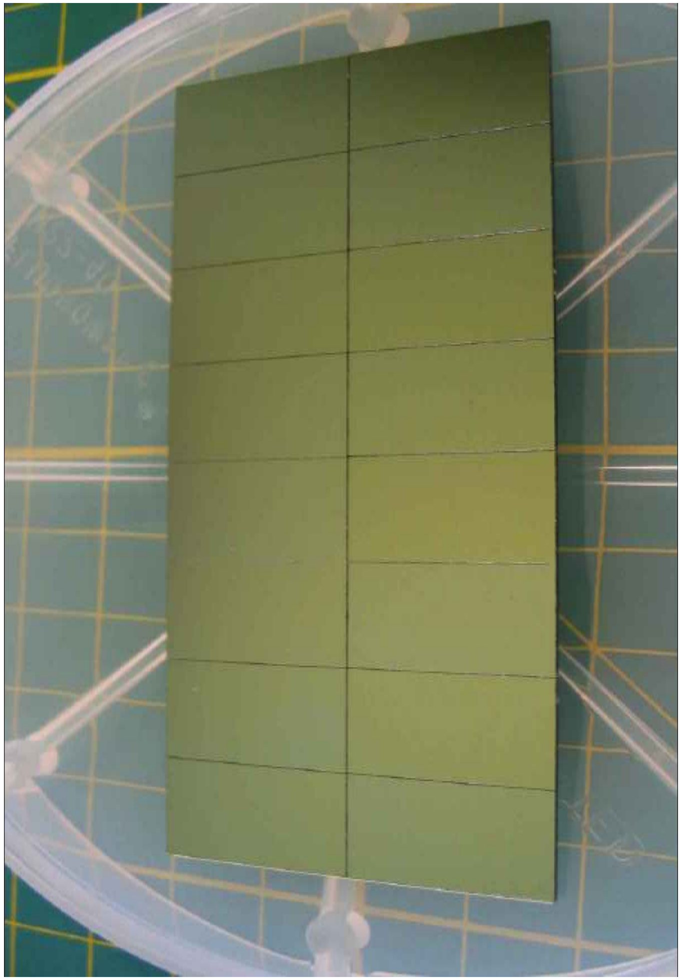

PILATUS II Active Pixel Chip

- Improvement of the PILATUS I Chip
- Radiation hard design

- 60 x 97 pixels = 5820 pixels
- Pixel size 172 x 172 um^2
- 17.540 x 10.450 mm^2

- Count rate: 1MHz/pixel
- 20 bit counter/pixel (1’048’575 X-rays)
- 6 bit DAC for threshold adjustment
- Read-out time= 2 ms

Detector chip fabricated by Hamamatsu

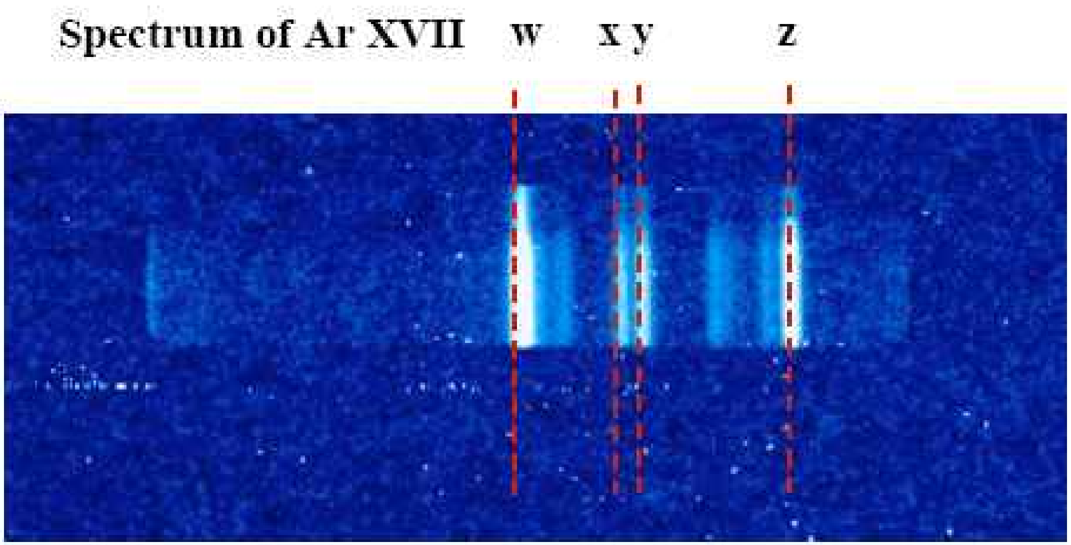

w: 3.9494 Å

x: 3.9661 Å

y: 3.9695 Å

z: 3.9944 Å

The raw data image of a spectrum from helium-like argon, ArXVII, that was obtained with a PILATUS II detector module.

Sensitivity to background radiation, including neutrons, is low

Noise counts are easily handled by the fast-counting pixels

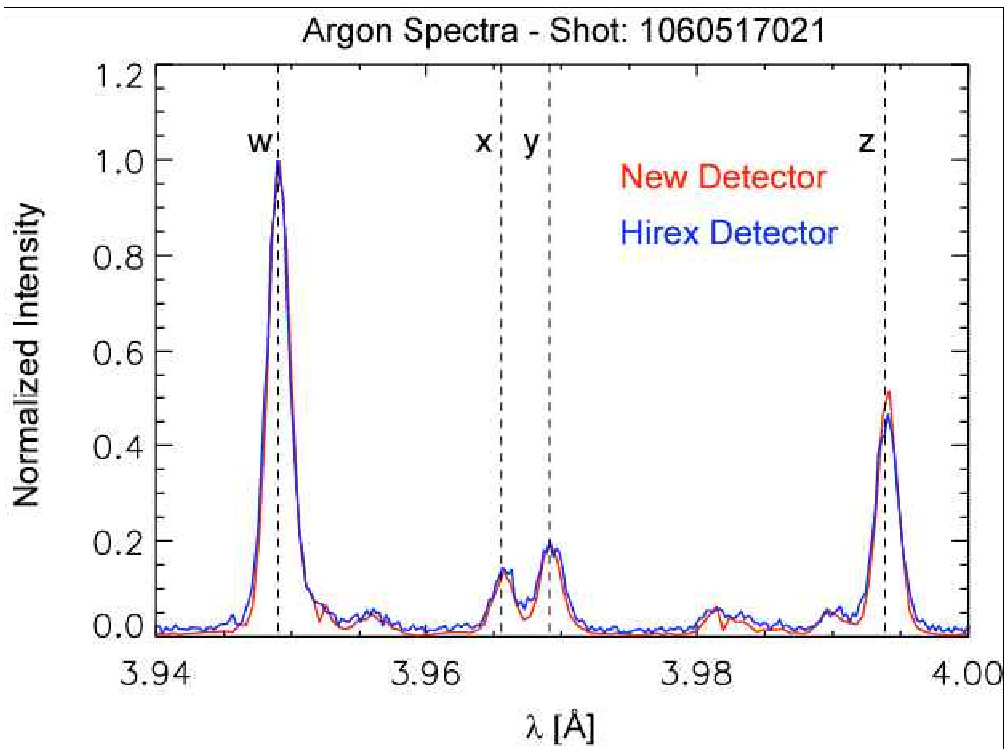

A comparison of ArXVII spectra, recorded with:

PILATUS II and a multi-wire proportional counter.

MEDIPIX2 Hybrid Pixel Detector

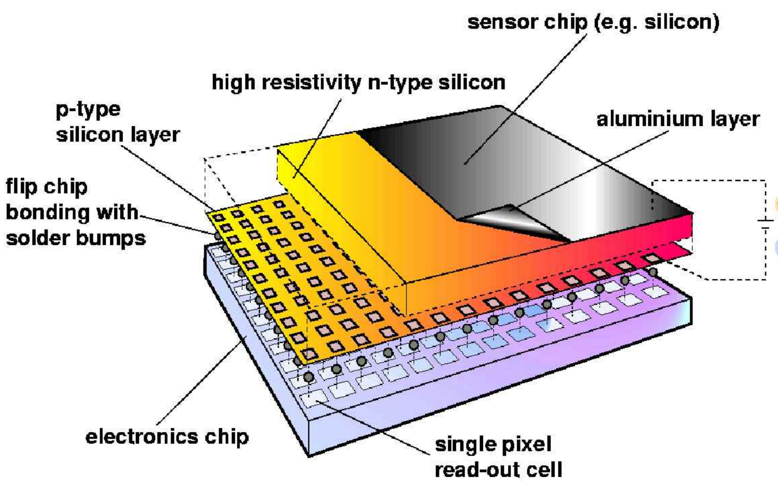

Detector and electronics readout are optimized separately

Medipix2 Cell Schematic

- Charge sensitive preamplifier with individual leakage current compensation
- 2 discriminators with globally adjustable threshold
- 3-bit local fine tuning of the threshold per discriminator
- 1 test and1 mask bit
- External shutter activates the counter
- 13-bit pseudo-random counter
- 1 Overflow bit

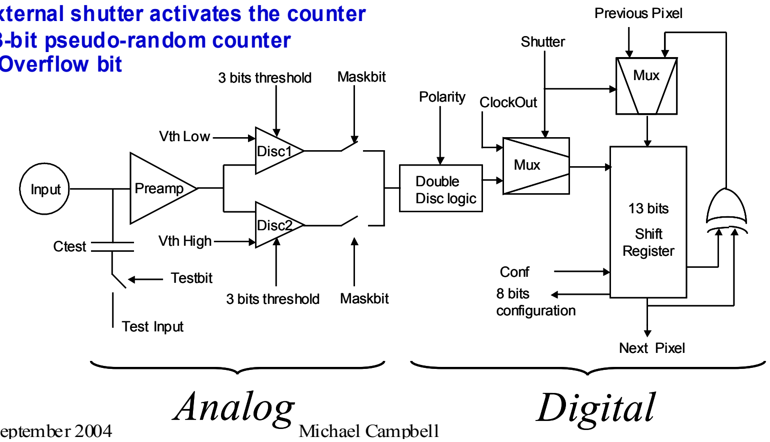

Medipix2 Cell Layout

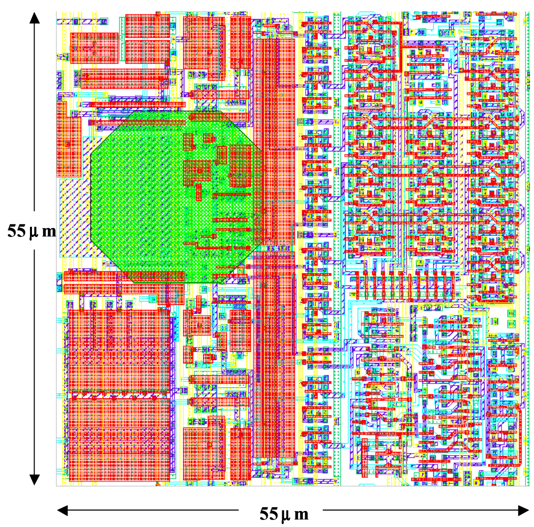

Medipix2 Chip Architecture

256 x 256 pixels
3ms readout time

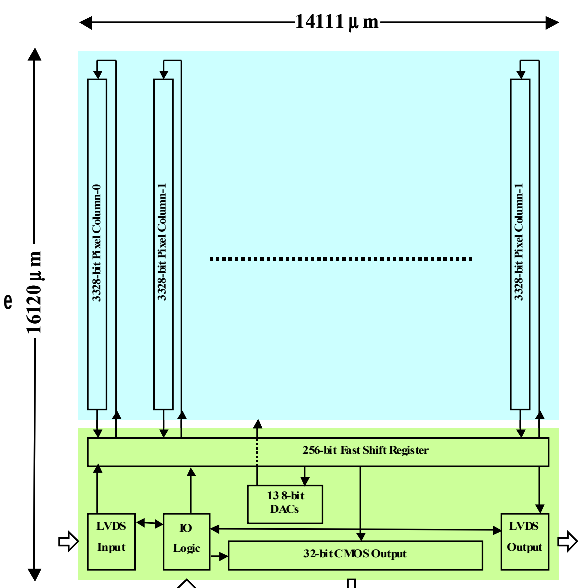

The revolution in x-ray/particle detectors

CERN Medipix II active pixel detector

Applications:

- X-ray imaging PHA
- Imaging X-ray crystal spectrometer
- Counting heavy ion beam probe
- Compact (imaging?) NPA

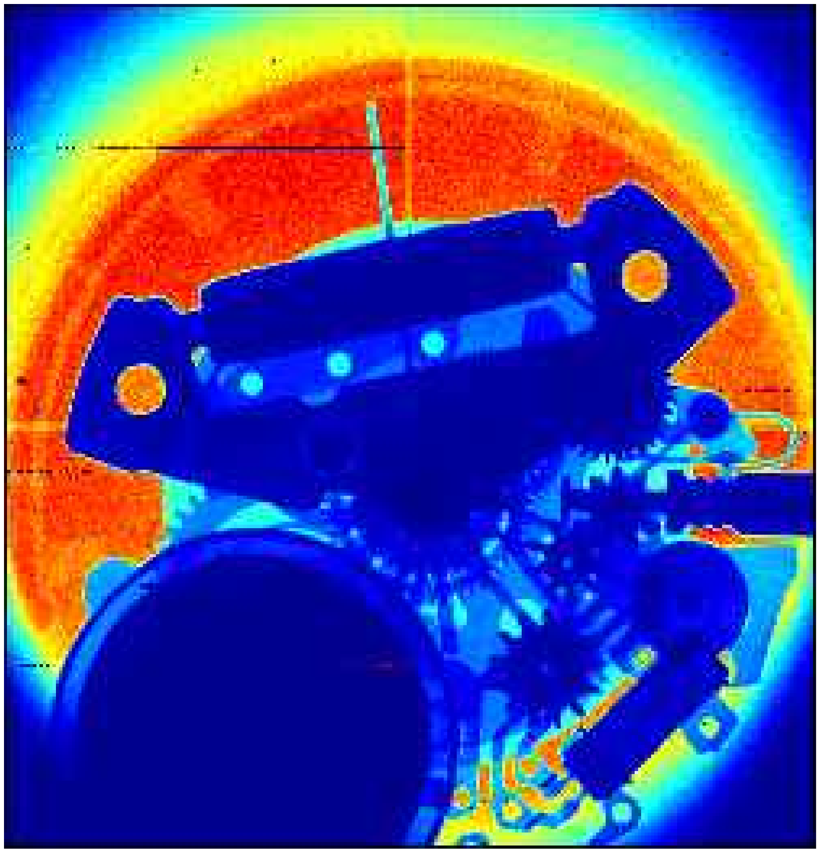

Medipix II in 2 x 2 array

Photon-counting ~ 5% energy-window at ~20 keV

Medipix II with USB interface

Medipix 3 – in development

- CMOS pixel detector readout chip designed for connection to a segmented semiconductor sensor.
- **"Colour" imaging** and dead-time free operation.
- Mitigation of charge-spreading by summing charge between neighbouring pixels and allocating the sum or hit to the individual pixel with the highest collected charge.
- Each pixel will have 2 thresholds and 2 counters, allowing simultaneous read/write mode (one counter is read out while the other counts).
- Sequential read/write mode with 2 different thresholds.
- Spectroscopic mode - Bump bond only 1 pixel in 4 - Pixel pitch increases from 55 um to 110 um - **8 thresholds and counters per pixel.**

Diagnostic applications for imaging energy-resolving detectors

No single detector fulfils all our requirements yet,
Developments are fast, and existing detectors are sufficient for R&D

- Direct x-ray imaging
- Crystal spectroscopy
- Soft x-rays 100 eV to 1keV
- VUV 10 eV to 100 eV
- Low energy and thermal neutrons
- Hydrogen isotopes and alpha particles
- Heavy ions
- Gamma ray imaging and spectroscopy

Neutronics modelling for diagnostic design and integration

Sam Davis(1), Robin Barnsley, Raul Pampin(1)
(1) UKAEA Culham

Attila neutronic analysis of the ITER imaging X-ray spectrometer to determine the best system architecture for the instrument.

The geometry was prepared in CATIA specifically for Attila such that one model could represent many possible design variations.

Acceptable limits on where detectors could be placed in terms of instrument life and signal-to-noise ratio have been identified.

The resulting design comprises three spectrometers located inside equatorial port 3 and one behind upper port 9 for each of the radial and toroidal arrays.

This allows complete coverage of the plasma minor radius without the use of graphite reflectors as in previous designs.

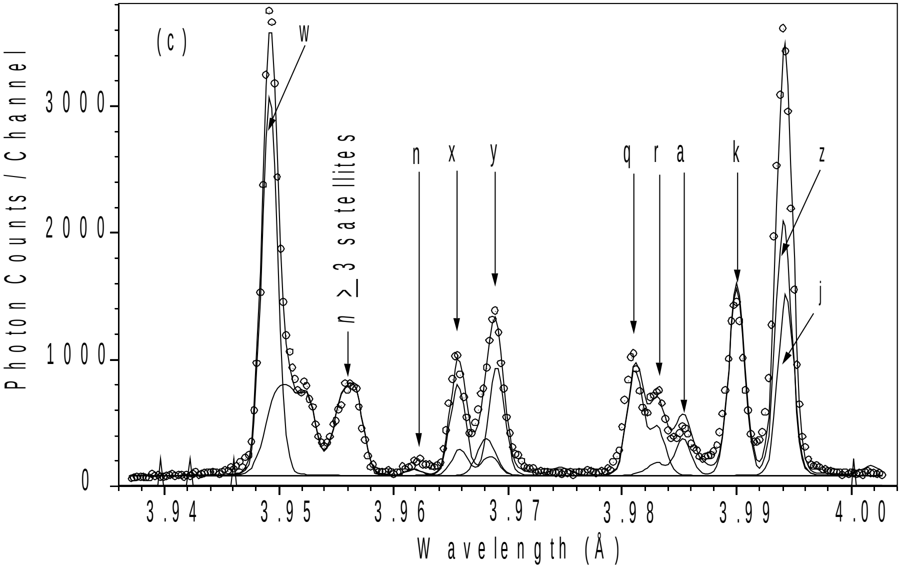

Te = 0.58 keV from <u>all</u> diel. satellites & line **w**; Ti = 0.45 keV

ArXVII spectrum from NSTX - Manfred Bitter

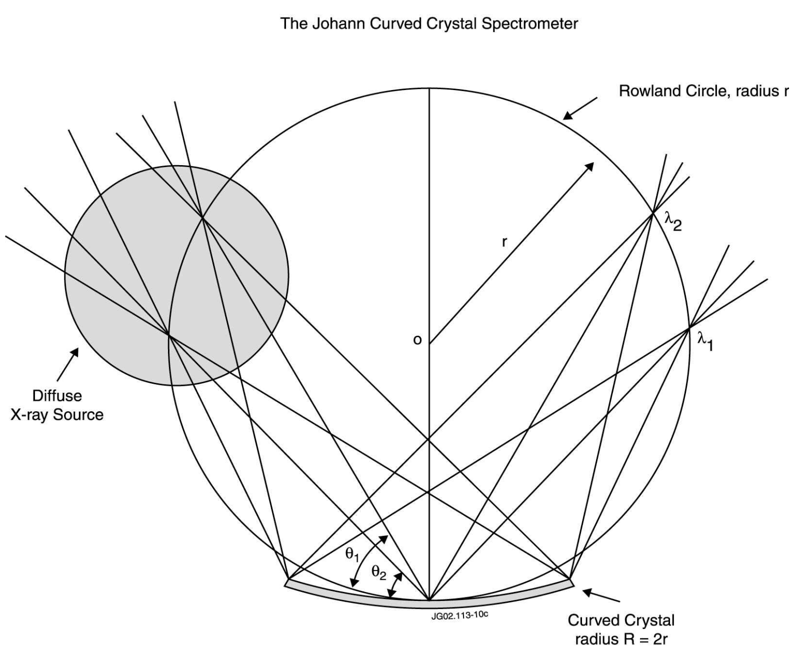

High-resolution x-ray spectroscopy

Extensively, but not exclusively, He-like ions.

~Te/Z: 250eV: Ne, 500eV,:Ar, 2keV: Fe-Ni, 10keV:Kr

Requires $\lambda/\delta\lambda$ >~ 5000, hence λ < 1.3 nm for crystals

Ti:	Doppler broadening		
Vtor/pol:	Doppler shift		
Te	Dielectronic satellite ratio		
ne	Forbidden line ratio z/(x+y) (sometimes)		
Zeff	Continuum	τimp	Impurity injection
nimp	Absolute calibration		

Simple and reliable - bent crystal & pos. sens. detector.

Crystals are cheap dispersive elements, eg Si < 1kEur

Energy resolving detector makes it doubly dispersive, with excellent signal-to-noise ratio.

All crystal-window-detector processes are volume effects, leading to calculable and stable calibration. (1 mm Carbon ~ transparent at 10 keV).

Detector developments have been the key to progress:

1st gen.	Photographic film
2nd gen.	Multiwire prop. counter, ~ 3 - 25 m radiius
3rd gen.	Solid state eg CCD, 0.5 - 2 m radius
4th gen.	**Imaging with fast 2-d detector**

ITER impurity line emission and spectrometer signals

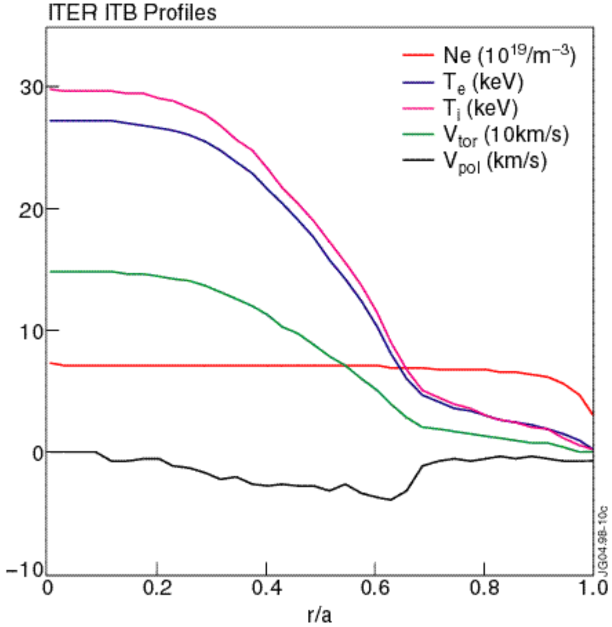

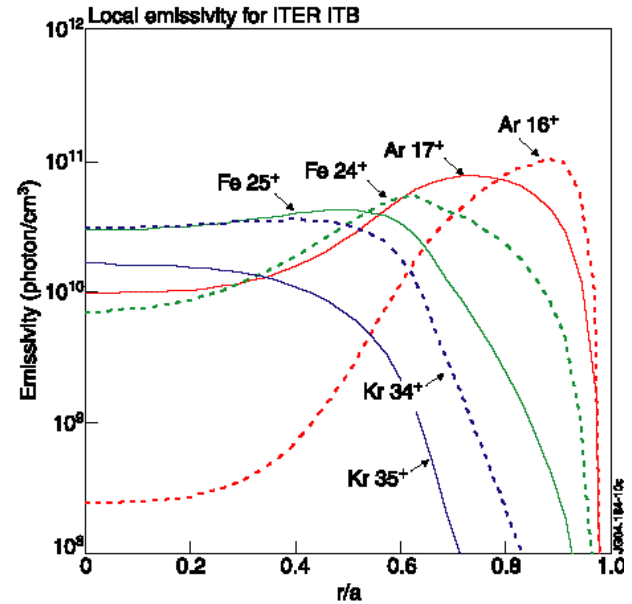

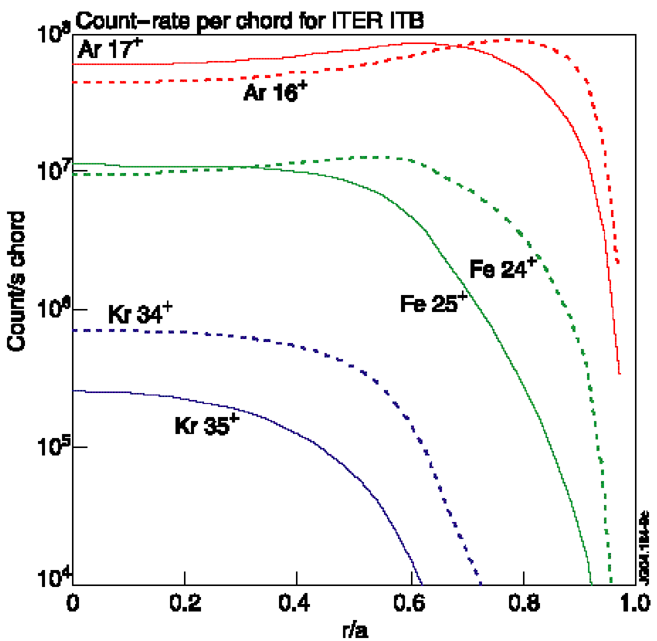

Top left Modelled ITER radial profiles

Top right Local emissivity of impurity spectral lines

Bottom Simulated signals for imaging x-ray crystal spectrometer

Incremental radiated powers for added impurity concentrations of $10^{-5}.n_e$ are:

Ar 0.25 MW Fe 0.8 MW Kr 1.4 MW

ITER imaging x-ray spectrometer

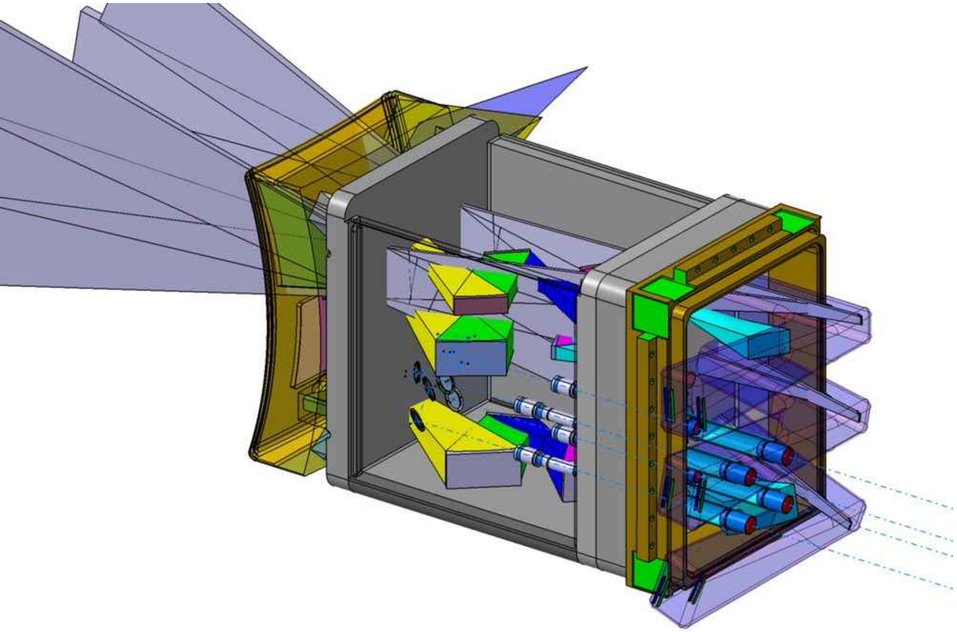

Design options for spectrometer location

- Ex-port

  Better access

  Better shielding

- In-port

  Wider view of plasma

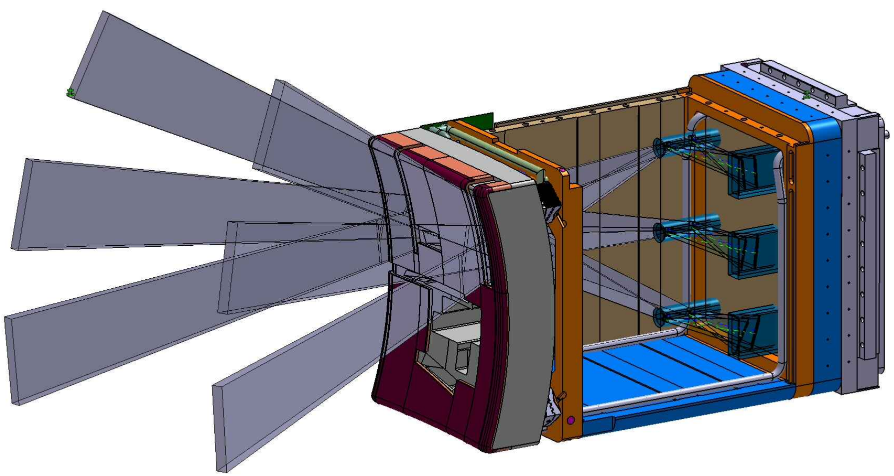

Choice will be based on:

- Neutronics modelling
- **Detector radiation hardness**
- **Detector background rejection**

The Jet Vacuum Spectroscopy Beamline

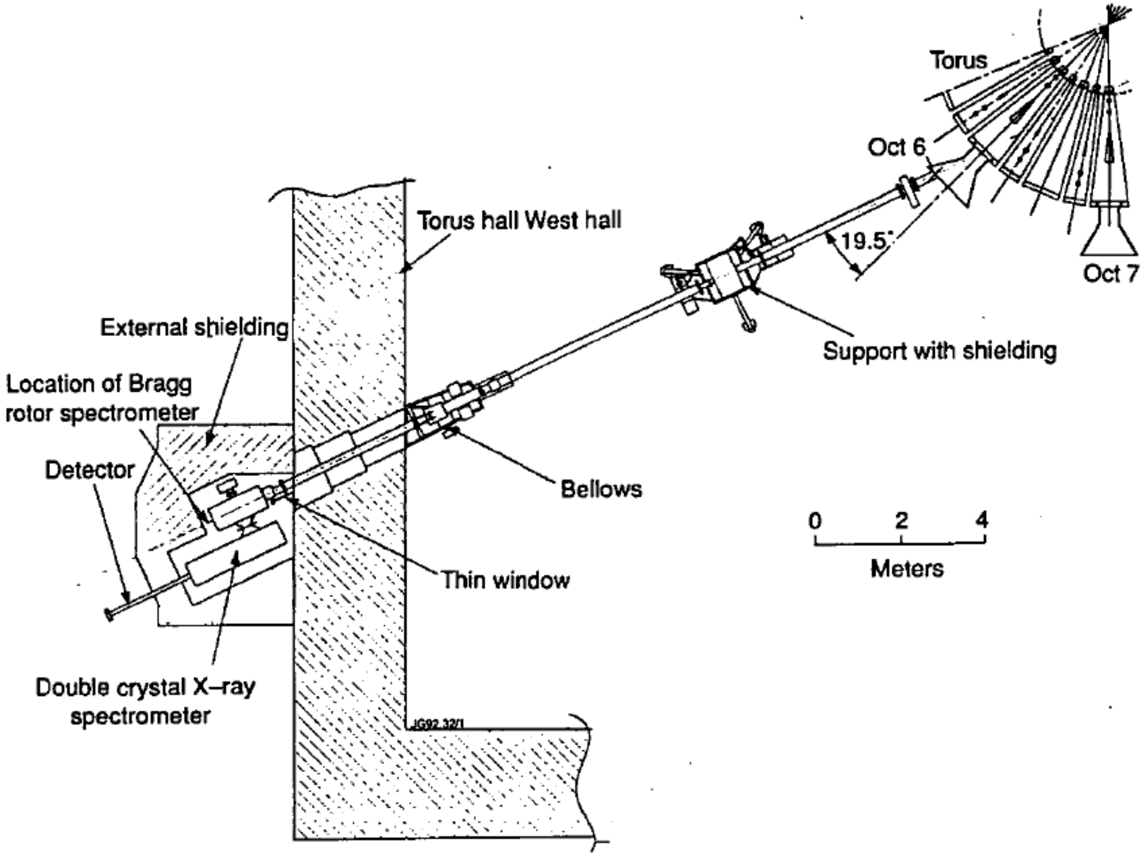

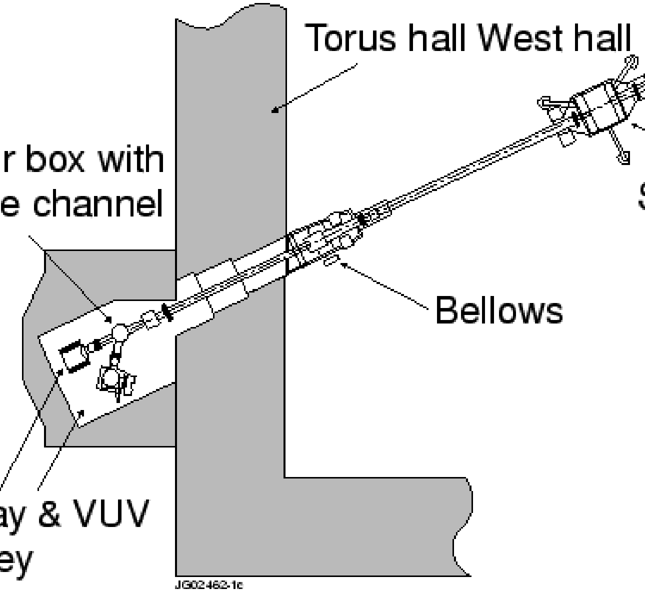

1988 - 1997

Double-crystal survey spectrometer

0.05 – 2.5 nm, crystals

Extremely conservative shielding and neutronics

High cost and complexity

Relatively slow and insensitive

Late delivery and commissioning

1998 – to date.

ITER-prototype

Soft x-ray survey spectrometer
0.05 – 10 nm, crystals and multilayers.

VUV spectrometer
10 – 100 nm, collimating mirror > grating.

Visible spectrometer
400 – 800 nm, mirror > telescope > optical fibre.

CATIA model prepared for input to *Attila*

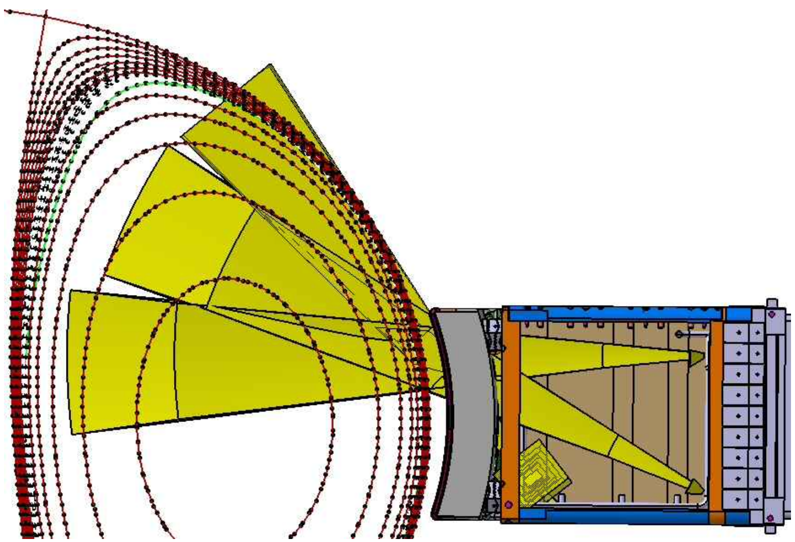

Plasma coverage by radial views

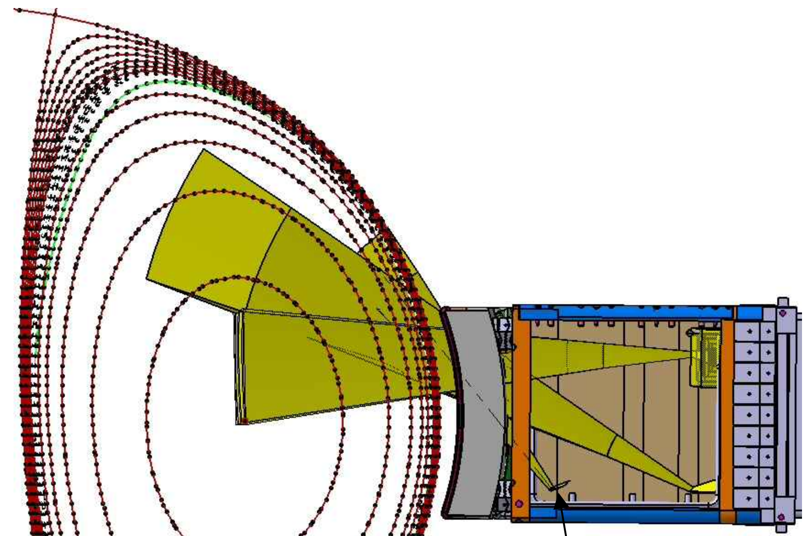

Plasma coverage by toroidal views

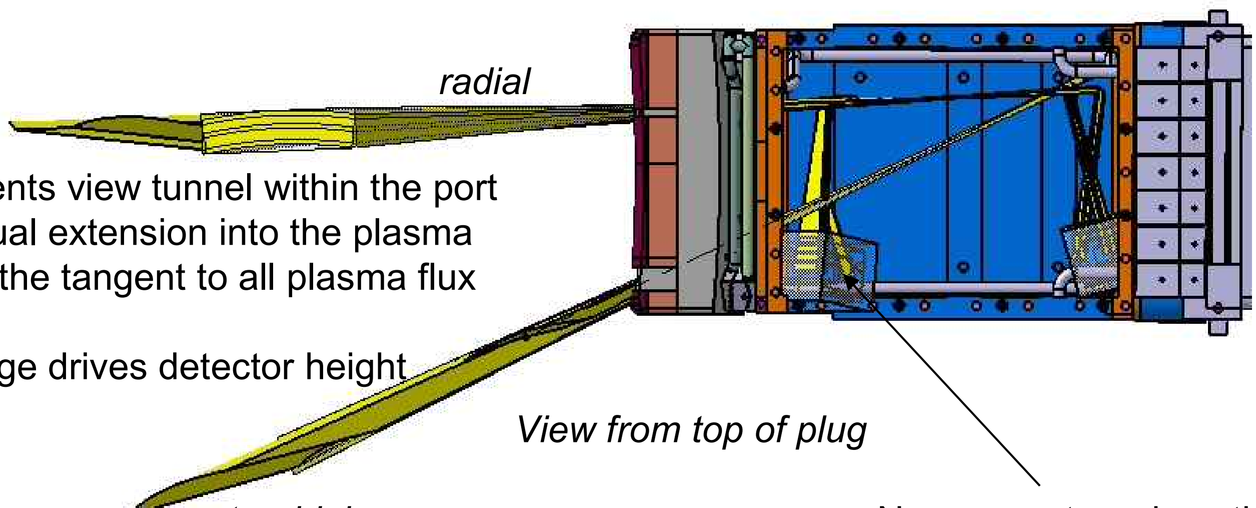

- Yellow represents view tunnel within the port plug and its virtual extension into the plasma
- Aim is to view the tangent to all plasma flux surfaces
- Spatial coverage drives detector height

Necessary to reduce the crystal-detector distance for the furthest-forward toroidal view spectrometer

Parametric CAD model of spectrometer, with options for input shielding and detector shielding.

crystal

detector

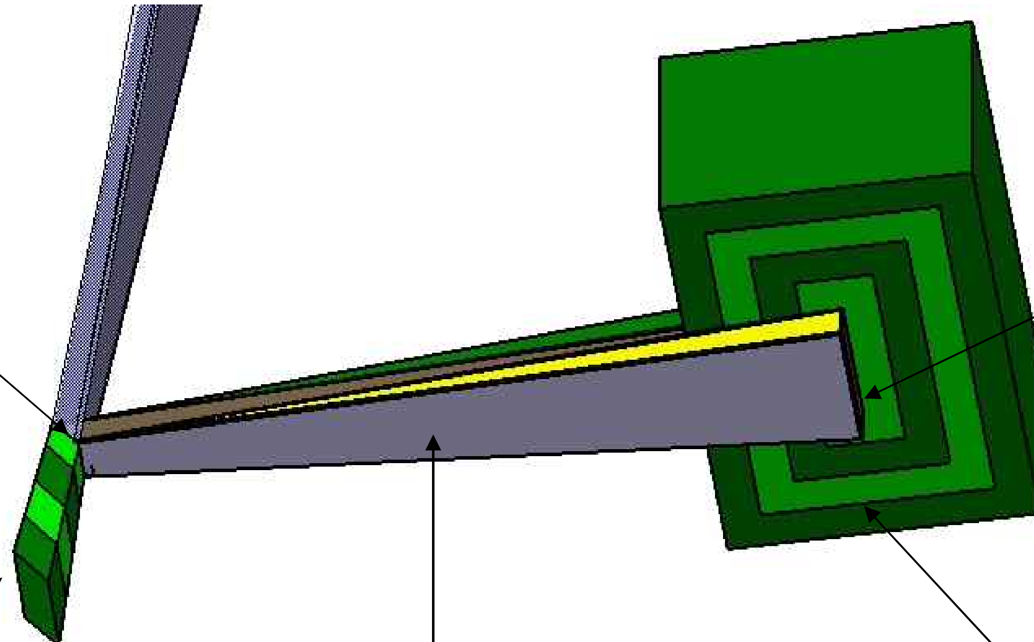

Option to model extended vacuum or neutron absorbers behind crystal to avoid direct line-of-sight scattering into the detector

Different widths for tunnel to detector for ±2° tuning – again modeled as adjacent layers

Different thicknesses of different materials around detector. Note these do not obstruct the tunnel between the crystal and the detector.
(section shown only)

Simplified CATIA model port-plug and spectrometers prepared for Attila

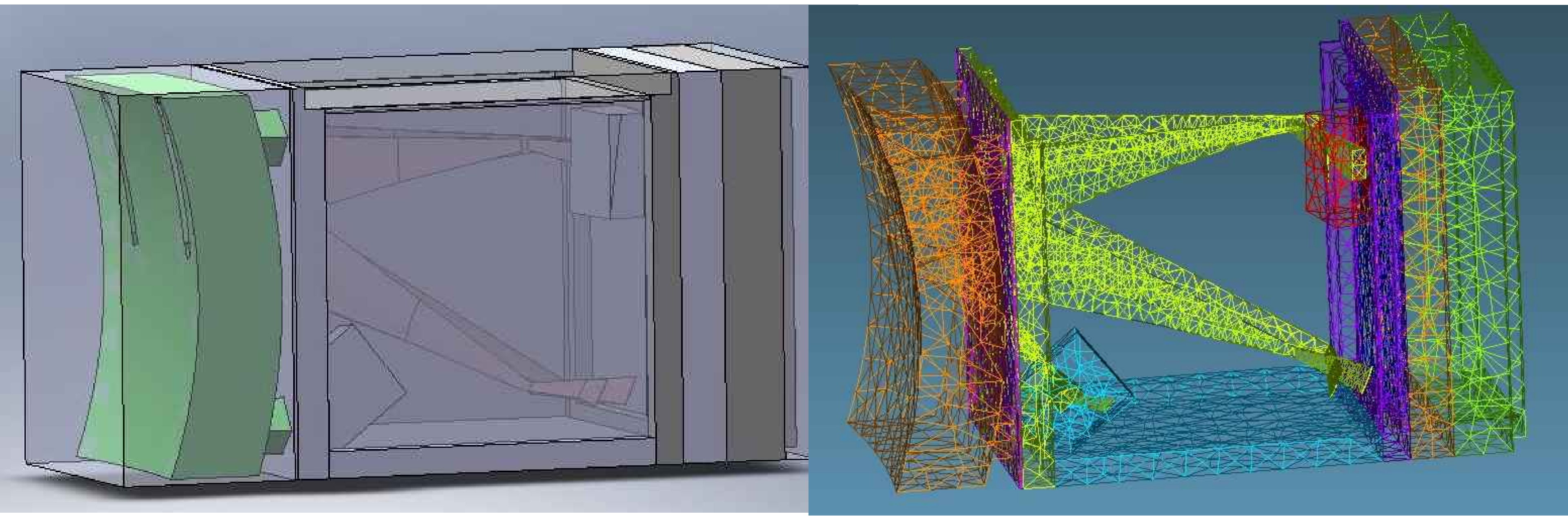

Neutron flux distribution, in log scale and per source neutron. XYZ in cm, origin at centre of ITER torus. Shield region and port walls removed to enable visualisation of the X-ray tunnels.

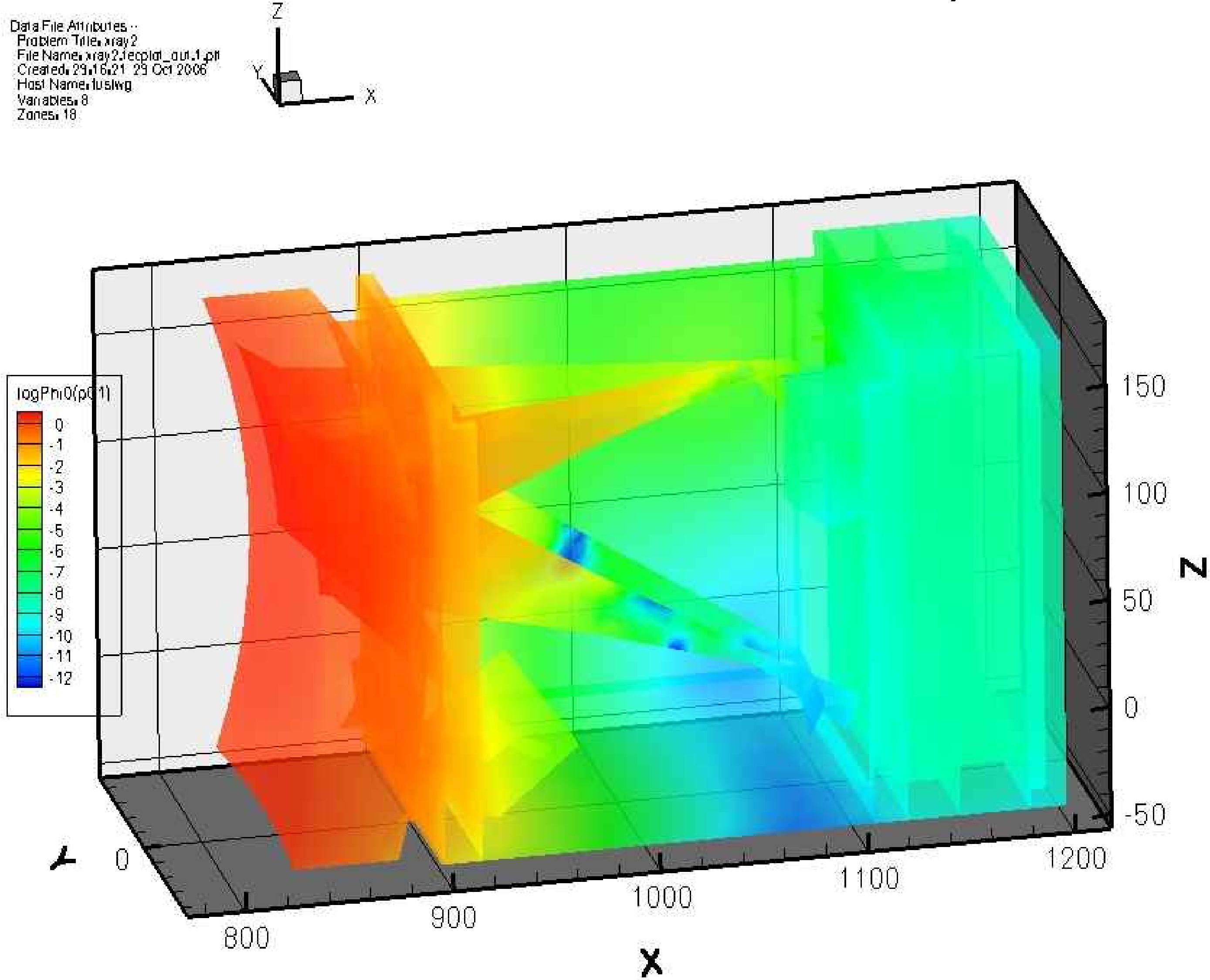

Z-plane cross section of the neutron flux, in log scale and per source neutron, at Z = 120cm (midplane of tunnels 1 and 3).

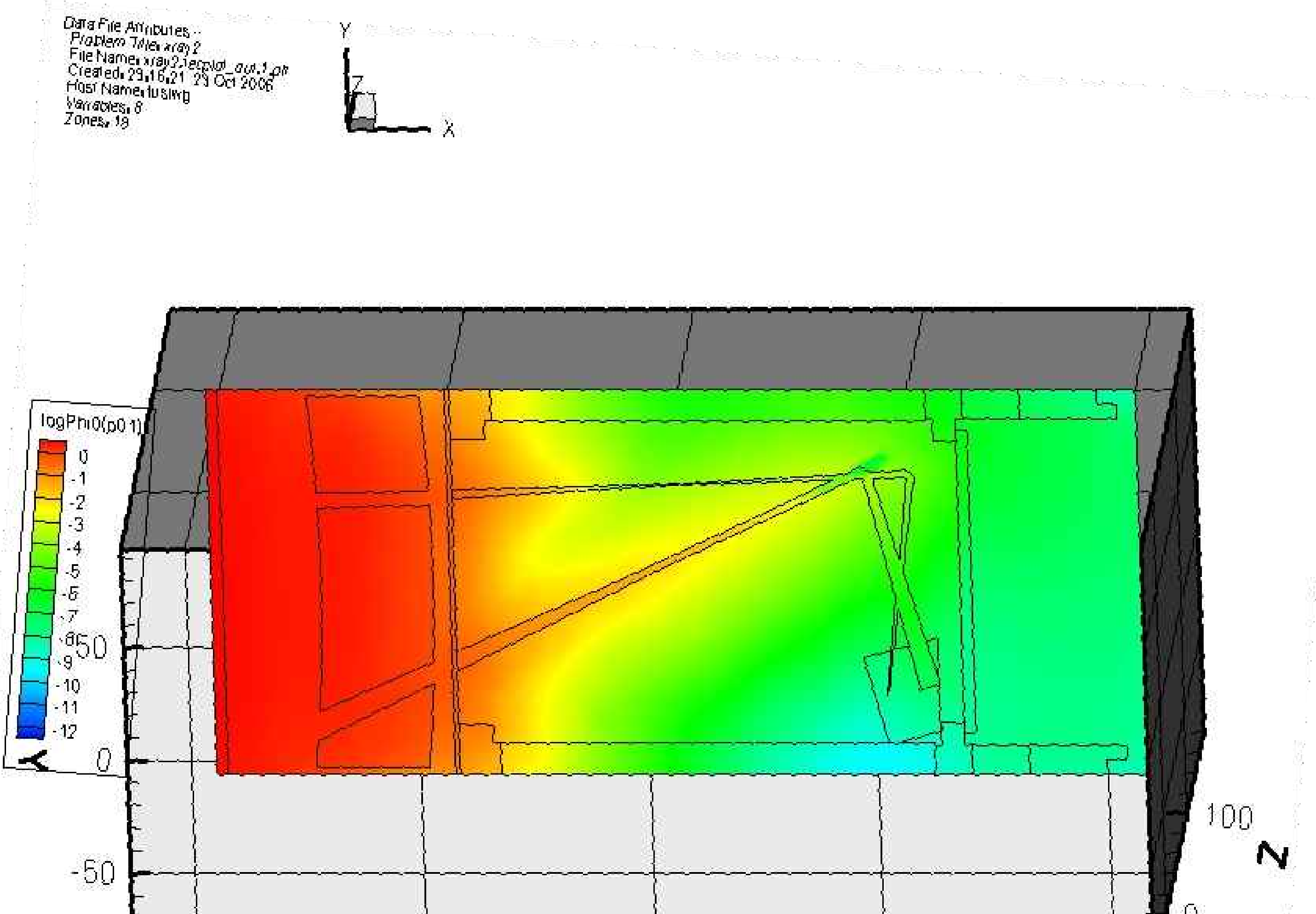

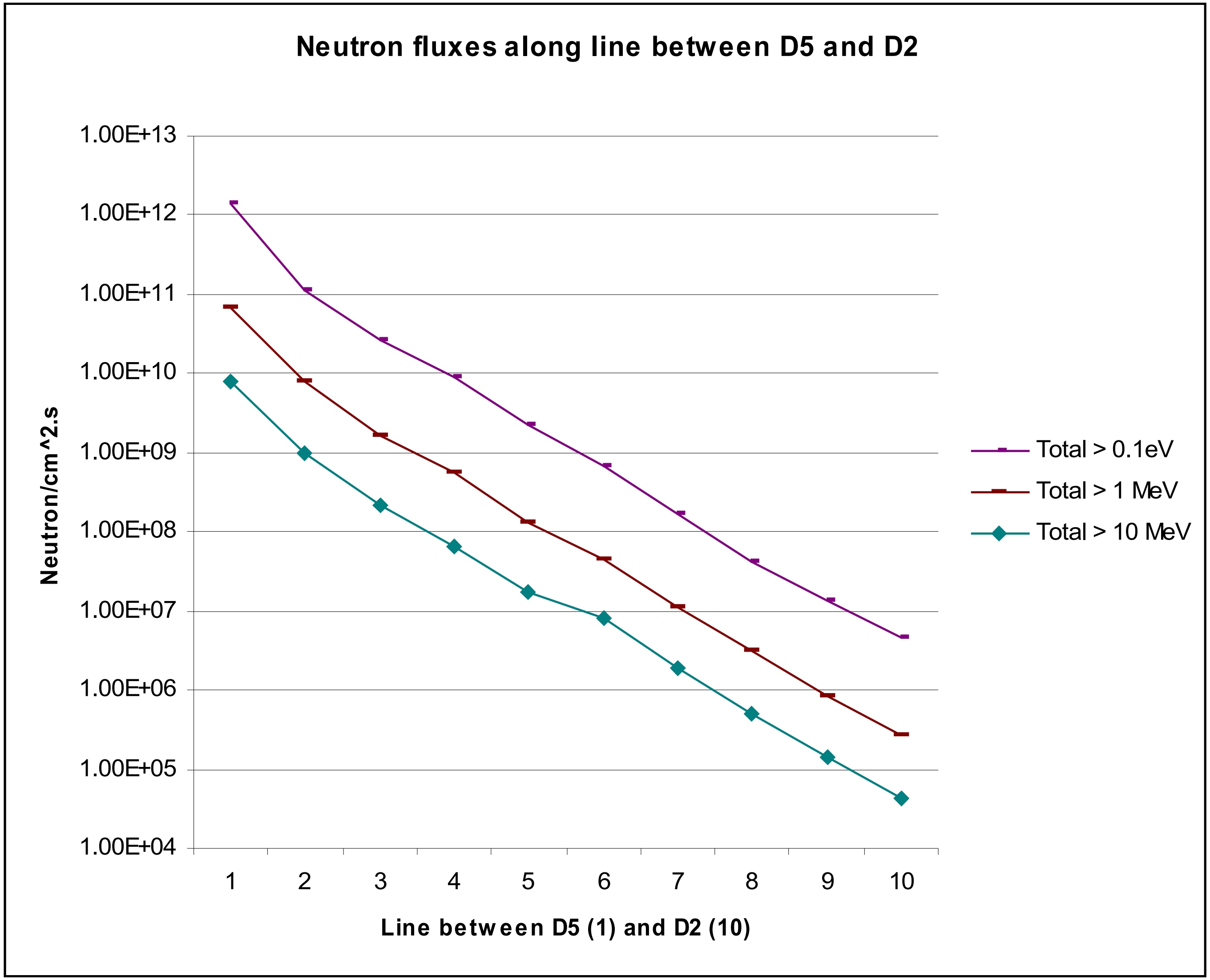

Neutron fluxes along line between D5 and D2
1.00E+13
1.00E+12
1.00E+11
1.00E+10
1.00E+09
1.00E+08
1.00E+07
1.00E+06
1.00E+05
1.00E+04
Neutron/cm^2.s
1 2 3 4 5 6 7 8 9 10
Line between D5 (1) and D2 (10)
Total > 0.1eV
Total > 1 MeV
Total > 10 MeV

Neutron spectra at the detector locations

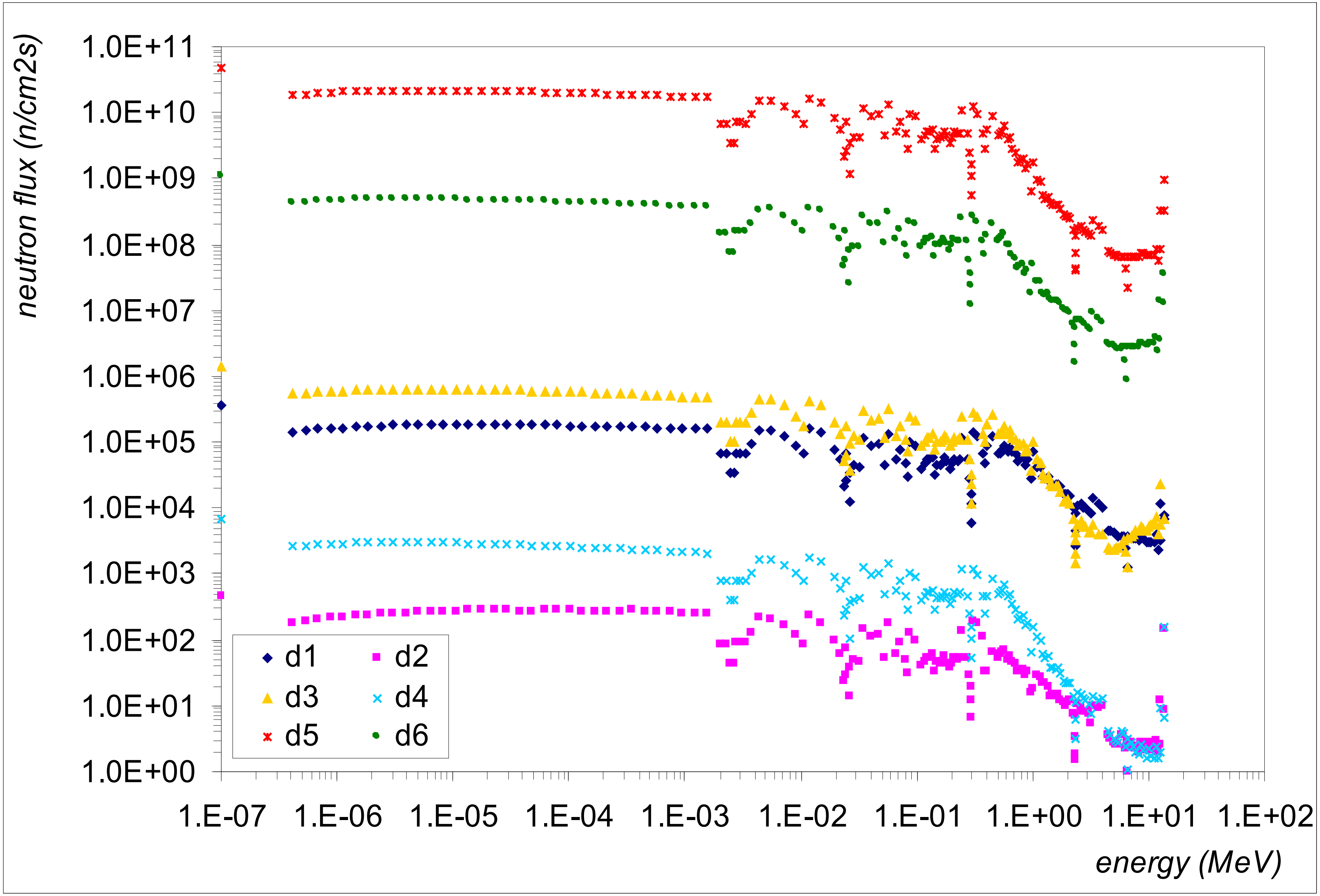

Photon spectra at the detector locations

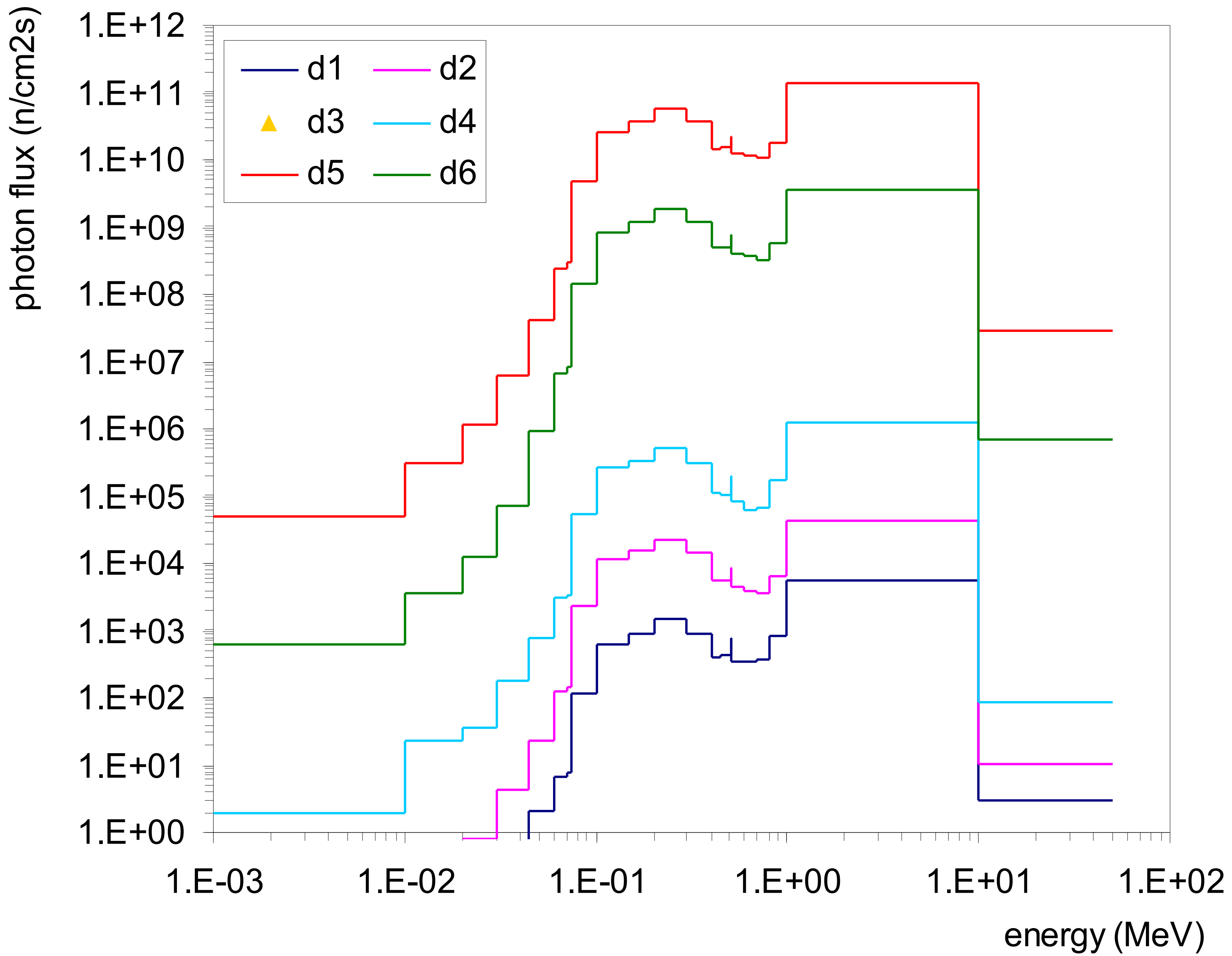

Table 9 Estimates of photon-induced background count-rates, assuming 1% QDE to gamma rays.

Detector location	Total gamma flux from fig.9 ($\gamma/cm^2.s$)	Total gamma count-rate For QDE-γ = 0.01 ($count/cm^2.s$)	Fraction of Medipix-II saturation rate ($3 . 10^{10} /cm^2.s$)	Fraction of Pilatus-II saturation rate ($3 . 10^9/cm^2.s$)	Photon background count-rate in 12-14 keV window ($count/cm^2.s$)
1	$3.22 .10^4$	$3.22 .10^2$	$1.1 . 10^{-8}$	$1.1 . 10^{-7}$	0
2	$3.22 .10^5$	$3.22 .10^3$	$1.1 . 10^{-7}$	$1.1 . 10^{-6}$	0
4	$8.75 . 10^6$	$8.75 . 10^6$	$3.7 . 10^{-5}$	$3.7 . 10^{-4}$	11
5	$1.00 . 10^{12}$	$1.00 . 10^{10}$	0.33	3.3	$1.5 . 10^5$
6	$3.06 . 10^{10}$	$3.06 . 10^8$	0.01	0.1	1800

Table 8 Estimates of neutron-induced background count-rates, assuming 1% QDE to neutrons.					
Detector location	Total neutron flux > 1 keV ($n/cm^2.s$)	Total neutron count-rate For QDE-n = 0.01 ($count/cm^2.s$)	Fraction of Medipix-II saturation rate ($3 . 10^{10} /cm^2.s$)	Fraction of Pilatus-II saturation rate ($3 . 10^9/cm^2.s$)	Neutron background count-rate in 12-14 keV window ($count/cm^2.s$)
1	$6.4 .10^6$	$6.4 .10^4$	$2 . 10^{-6}$	$2 . 10^{-5}$	Difficult to estimate
2	$7.2 .10^3$	72	$2.4 . 10^{-9}$	$2.4 . 10^{-8}$	
3	$1.5 . 10^7$	$1.5 . 10^5$	$5 . 10^{-6}$	$5 . 10^{-5}$	
4	$5.7 . 10^4$	$5.7 . 10^2$	$1.9 . 10^{-8}$	$1.9 . 10^{-7}$	
5	$5.3 . 10^{11}$	$5.3 . 10^9$	0.18	1.8	
6	$1.2 . 10^{10}$	$1.2 . 10^8$	0.004	1.3	

Table 7: Estimates of detector lifetimes due to neutron damage. 10^7s: ITER lifetime. 10^6s: maintainable			
Detector location	Flux >100 keV ($n/cm^2.s$)	Time for fluence of 10^{14} /cm^2 (s)	Time for fluence of 10^{16}/cm^2 (s)
1	$3.3 .10^6$	$3 . 10^7$	$3 . 10^9$
2	$2.9 .10^3$	$3.4 . 10^{10}$	$3.4 . 10^{12}$
3	$5.8 . 10^6$	$1.7. 10^7$	$1.7. 10^9$
4	$2.0 . 10^4$	$5 . 10^9$	$5 . 10^{11}$
5	$2.0 . 10^{11}$	**500**	**$5 .10^4$**
6	$4.9 . 10^9$	**$2 . 10^4$**	$2 . 10^6$

2. Windows and lens: Irradiation test results
K Vukolov, Kurchatov Inst.

KU-1 is the most reliable window material for ITER

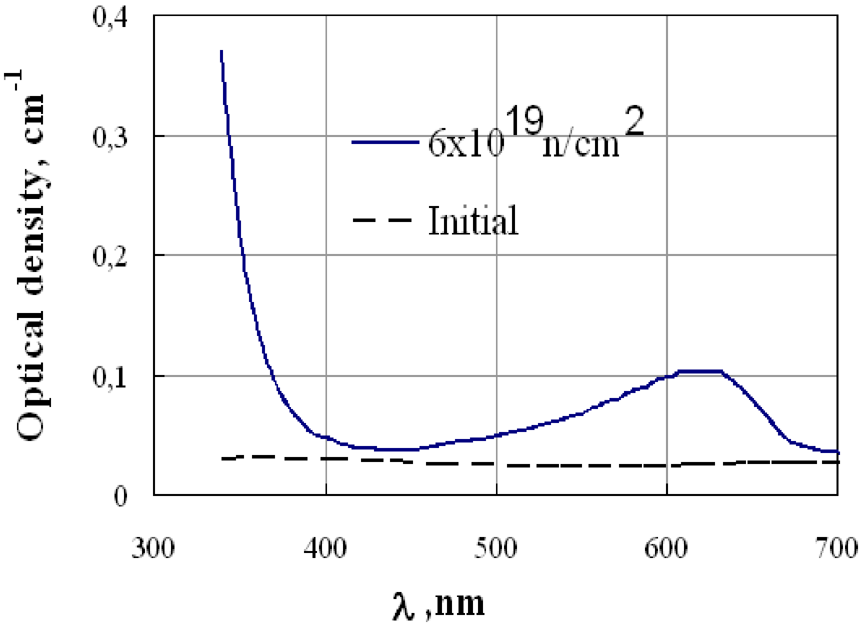

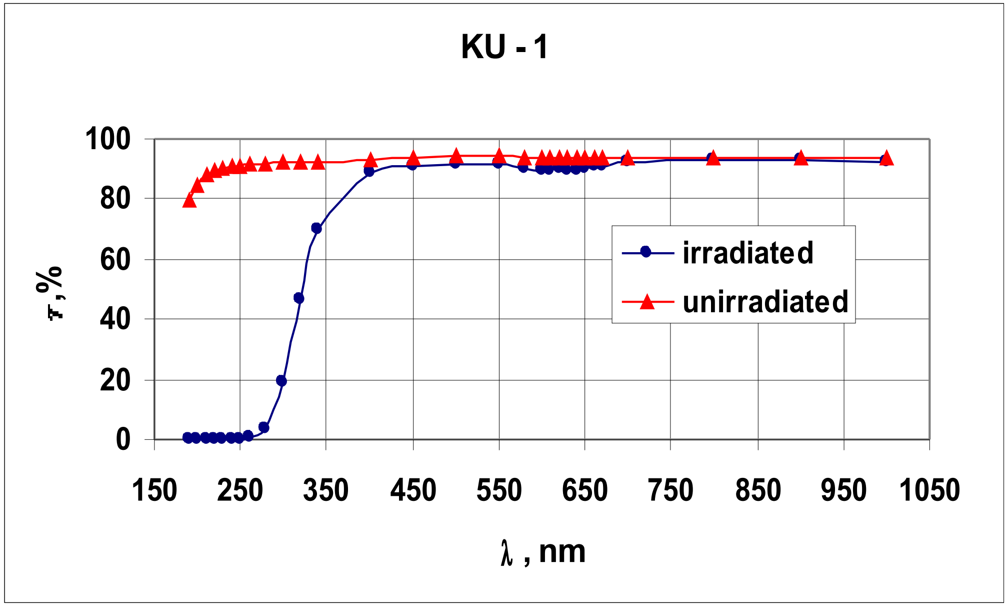

KU-1 optical density after irradiation in nuclear reactor at 55°C up to $F_{>0,1}=6\times10^{19}$ n/cm^2 and gamma dose about 2 GGy (Si) [4].

Transparency spectra of KU-1 silica glass (1 cm thickness) before and after irradiation in nuclear reactor at 30°C up to $F_{>0,1}=3\times10^{16}$ n/cm^2 and gamma dose about 1 MGy (Si) [3].

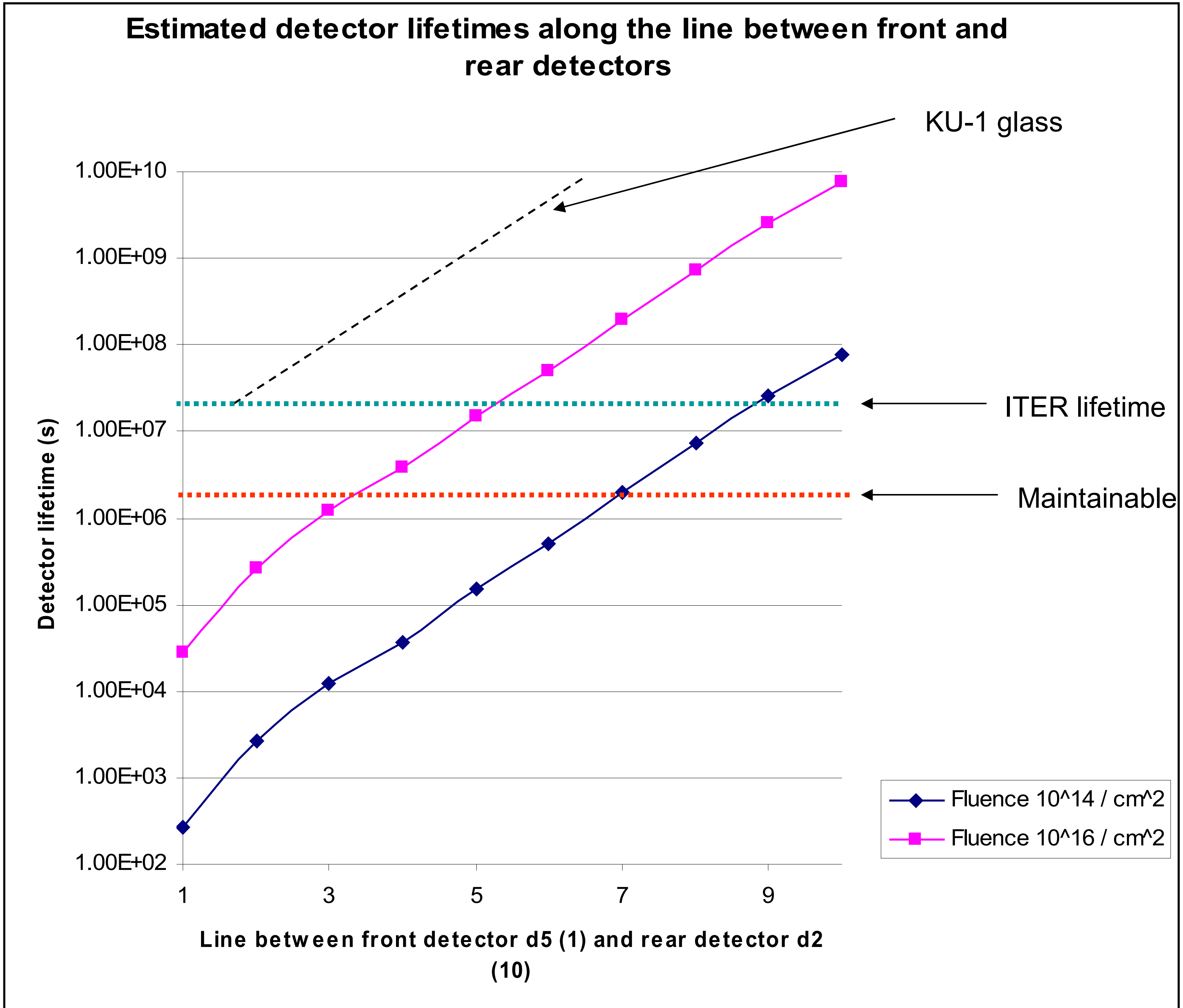

Estimated detector lifetimes along the line between front and rear detectors
KU-1 glass
ITER lifetime
Maintainable
1.00E+10
1.00E+09
1.00E+08
1.00E+07
1.00E+06
1.00E+05
1.00E+04
1.00E+03
1.00E+02
Detector lifetime (s)
1
3
5
7
9
Line between front detector d5 (1) and rear detector d2 (10)
Fluence 10^14 / cm^2
Fluence 10^16 / cm^2

Parametric CAD model to optimize positioning of Equatorial and Upper imaging crystal spectrometers

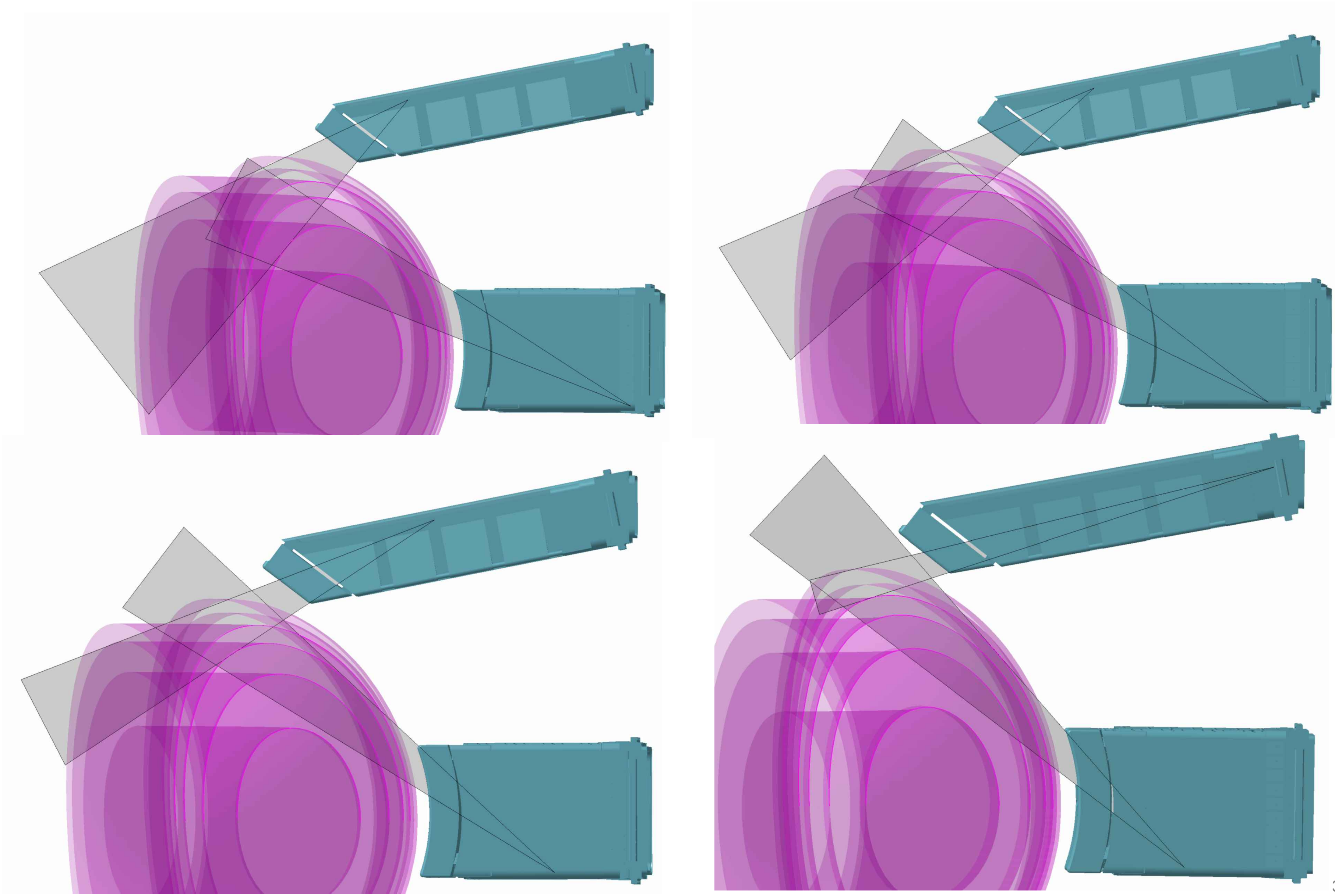

Discussion point for suggested broad equivalence of instrumentation between the 1998 and 2007 designs for the ITER crystal spectroscopy system

ITER 98	2007
XCS-Survey - 1 x single reflection survey spectrometer - 1 x double reflection survey spectrometer	**XCS-Survey + upper imaging** - 1 x single reflection survey spectrometer - 1 x imaging spectrometer at upper port*
XCS-Array 5 discrete chords - 5 x graphite reflectors in equatorial port - 5 x crystal spectrometers ex-port - 5 x 1-d position-sensitive detectors ex-port	**XCS-Array** Continous poloidal resolution for r/a < ~0.7 - 3 x imaging spectrometers in equatorial port - 3 x 2-d position-sensitive detectors in-port

*Further analysis and design study is required before deciding to move the upper imaging system inside the port, and at present we should keep the the 1995 design, with the spectrometer behind the port.

- Neutronics analysis similar to equatorial port
- Integration study – the space is quite small.

Summary

- Timely neutronics analysis will allow us to optimize diagnostic integration
  - CATIA model of generic equatorial port-plug, simplified for input to *Attila.*
  - Importing CATIA into *Attila* requires considerable work
  - *Attila* results are very useful

- Detector radiation hardness continues to improve.
  - Led by High Energy Physics, Synchrotrons, etc
  - Detector R&D, and future performance, is important for current design work.

- Windows and lenses can be considered within the port
  - Location depends on thickness, spectral range etc.
  - Could the vacuum boundary be moved forward in some cases?

- Optimized shielding will improve diagnostic performance, and may reduce cost and complexity.

The Way to Fusion Energy

ITER ex-vessel x-ray camera

Robin Barnsley(1) & Martin O'Mullane(2)

(1) Queen's University Belfast, EFDA/JET, ITER International Team, Cadarache, France.
(2) Strathclyde University and EFDA/JET

- Modelled broadband x-ray emission
- Principles of camera module
- Integration into Eq 09 and Up 09
- Modelled performance

Update of x-ray camera on Eq 09

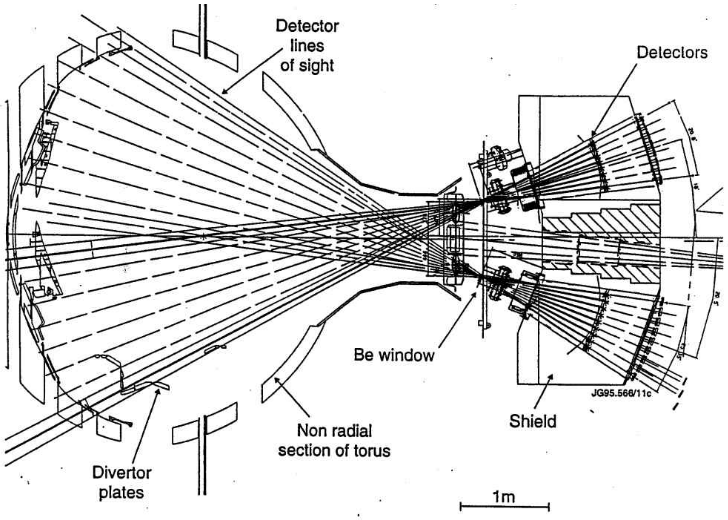

The JET D-T compatible soft x-ray camera

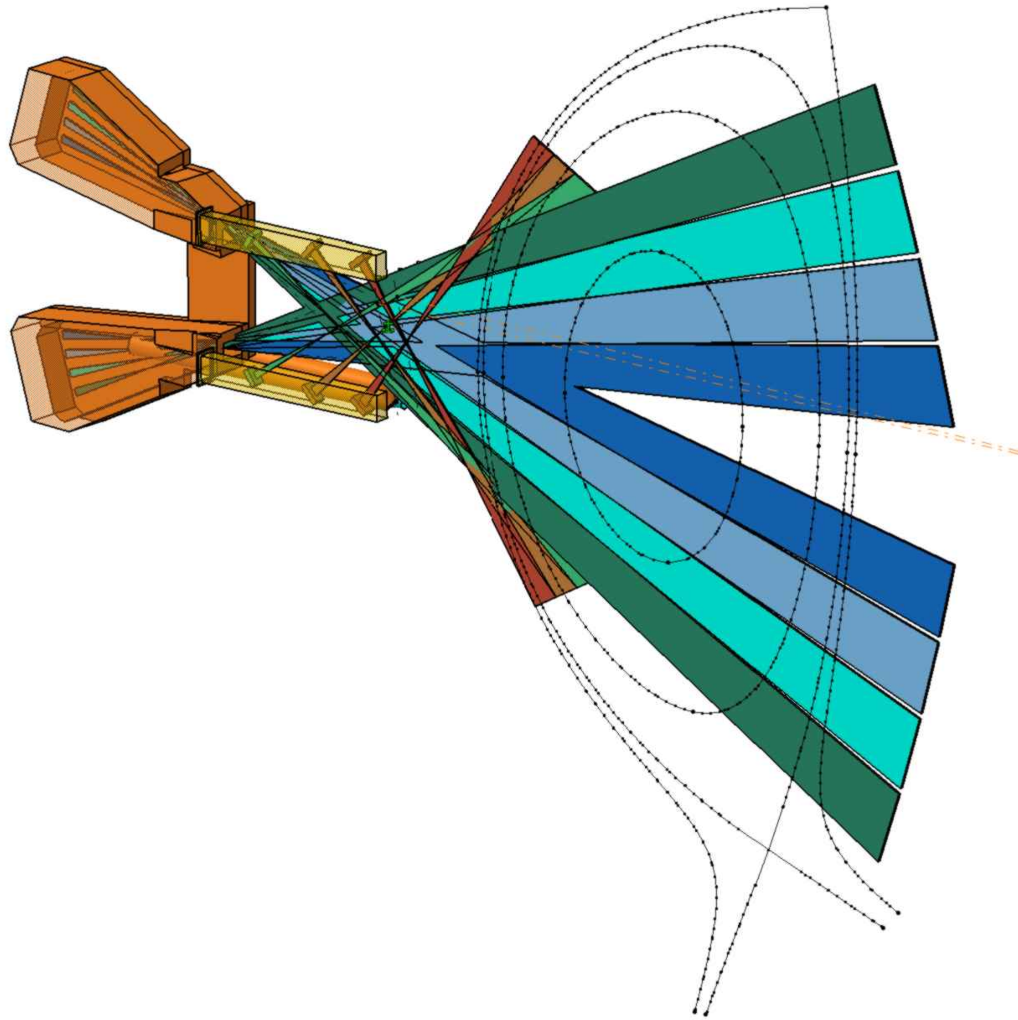

Continuous poloidal resolution

Outer plasma viewed by in-port detectors in removable cassettes

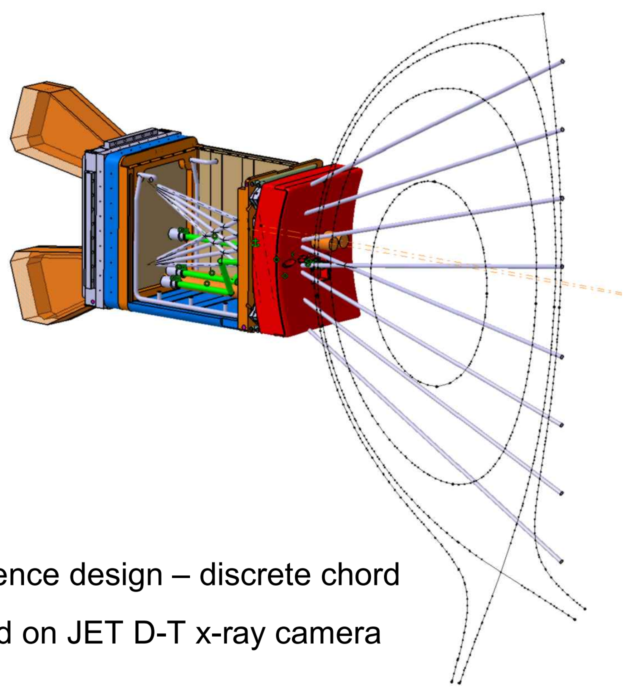

Reference design – discrete chord

Based on JET D-T x-ray camera

ADAS-SANCO modelled ITER broadband x-ray spectra

Line and continuum in 5% energy bands, radially resolved

< 10 keV: mainly impurity information

> 10 keV: mainly Te information

Modern detectors will be able measure this…

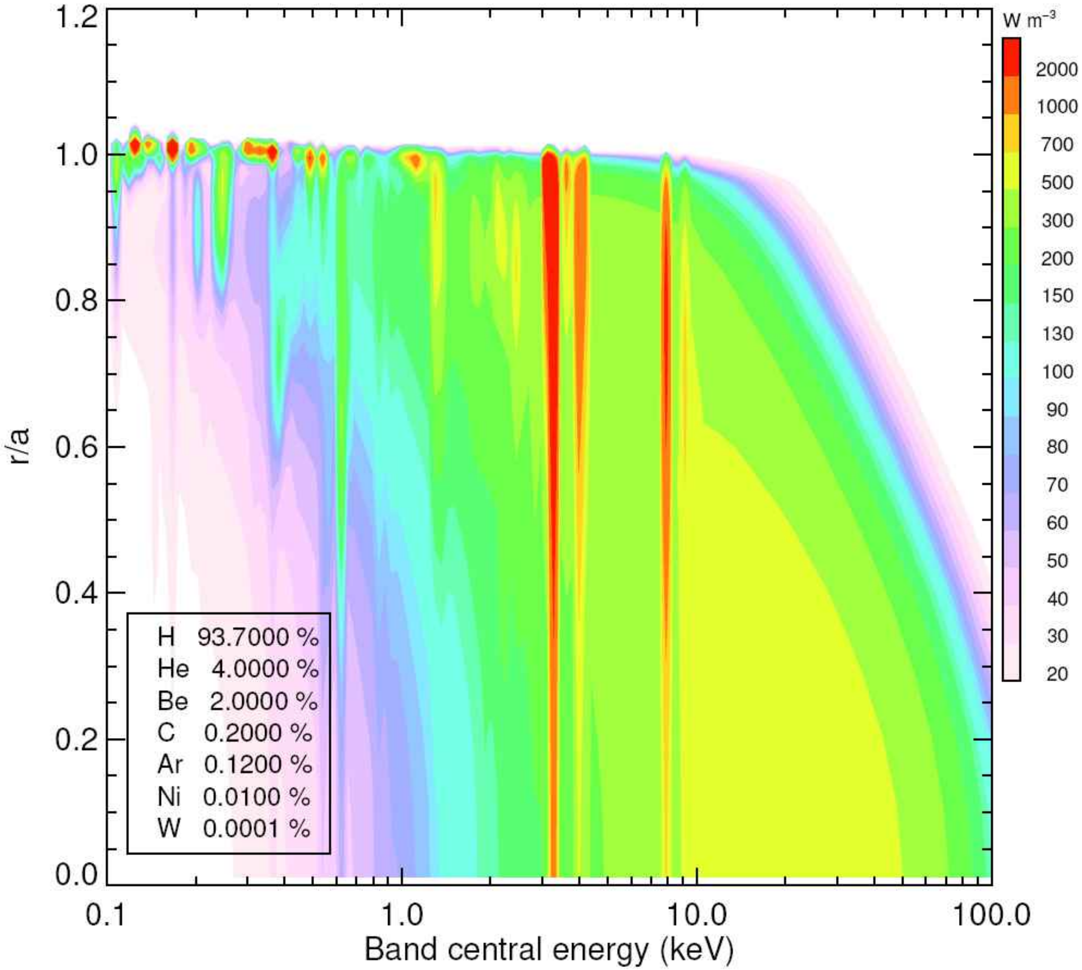

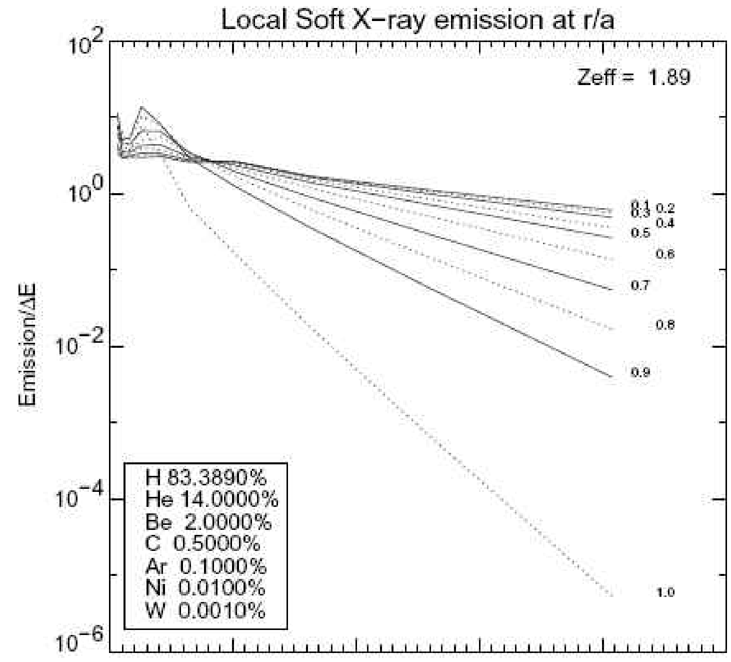

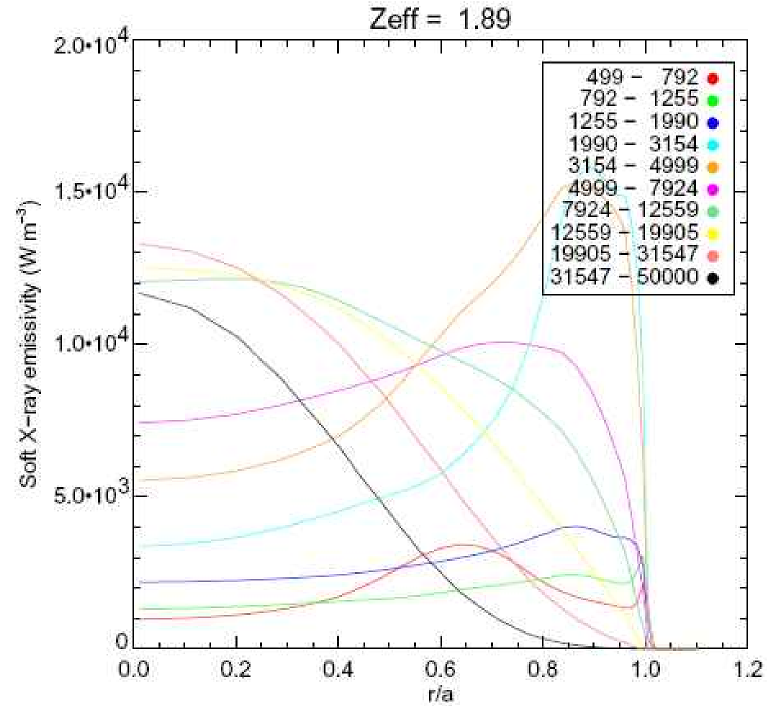

Outline parameters of ex-vessel x-ray camera module

- Narrow angle of view to maximize neutron shielding
- Window can be substantial eg 1-5 mm Be or 1-2 mm diamond
- Detector: Fast, radiation-hard, photon-counting, energy-resolving position-sensitive detector
    - eg CERN-Medipix, PSI-Pilatus, ENEA-Pacella

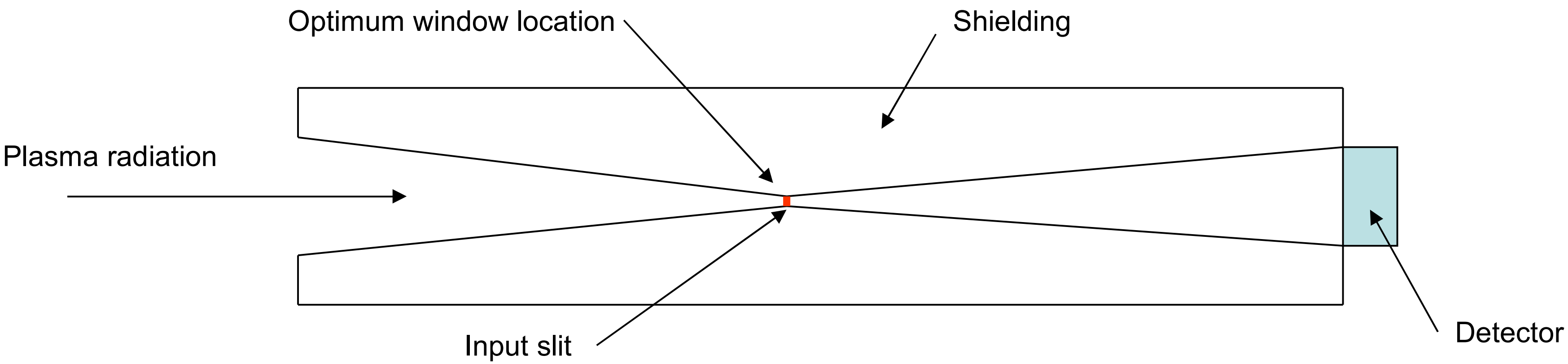

Outline dimensions		Detector performance	
- Entrance slit to detector:	~ 1 m	- 1d spatial resolution:	<~ 250 um
- Entrance slit to plasma:	~ 5 m	- Energy range:	1 – 100 keV
- Slit width x height:	1 x 5 mm^2	- Multi-channel energy resolution:	5 -15%
- Angle of view:	5 deg.	- Peak count-rate:	1.5 . 10^9 /cm^2.s
- Poloidal resolution for 1mm slit:	5 mm	- Peak neutron flux:	6 . 10^6 /cm^2.s
- Blanket slot width:	< ~20 mm	- Time for n-fluence of 10^14 /cm^2:	~ 10^7 s

Ex-vessel x-ray camera in Eq 09

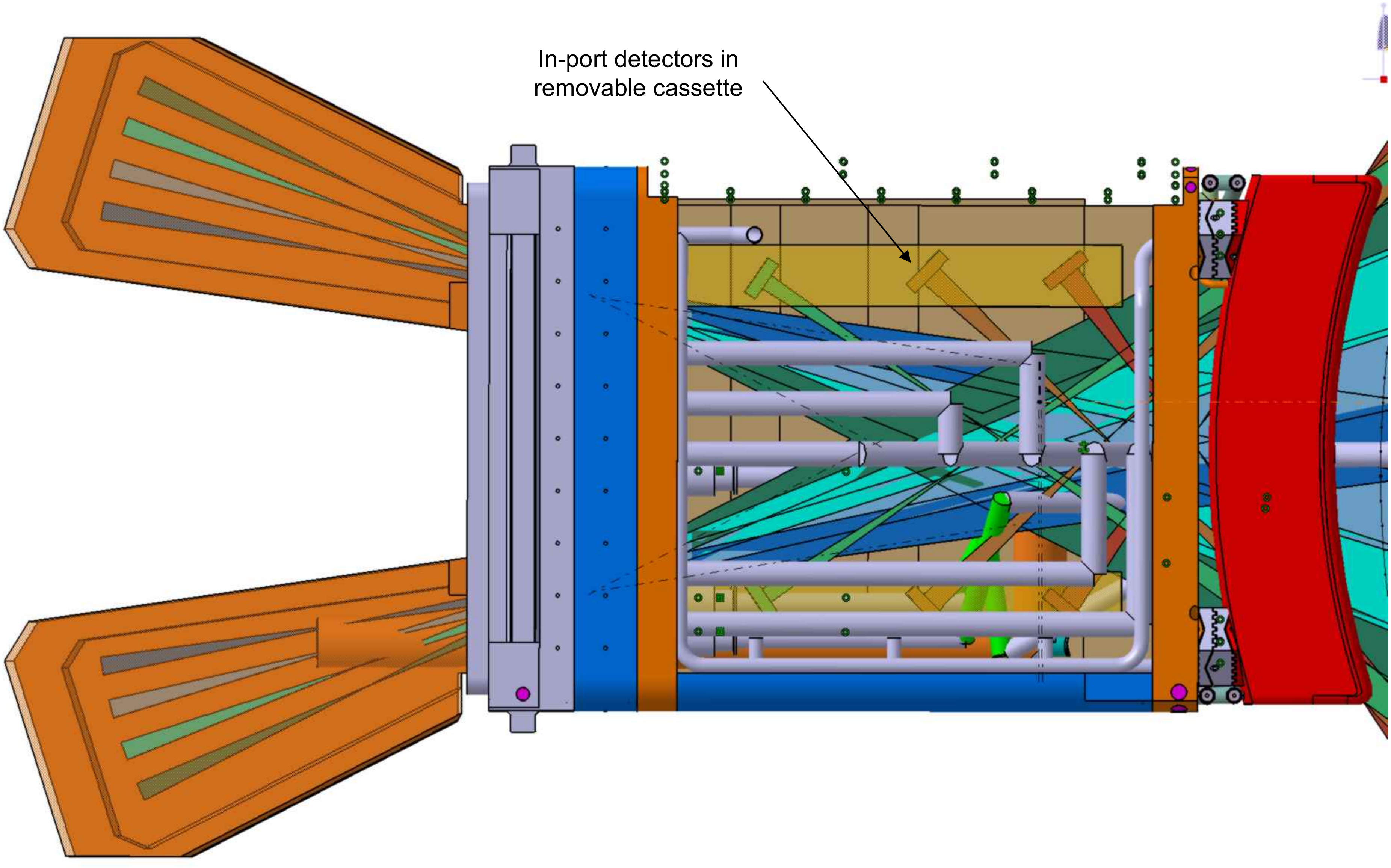

Signals, and emission reconstruction

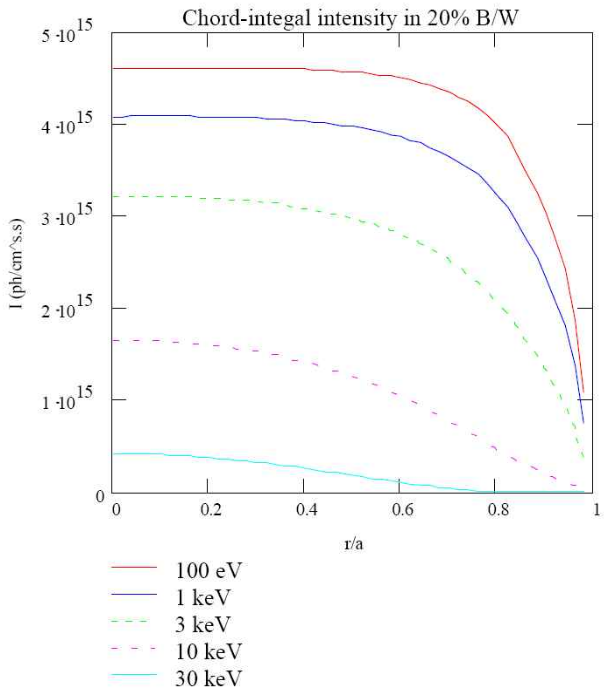

+ Instrument geometry
+ 1 mm Be window
+ Detector QDE
  (x-ray 0.5, and neutron 1.0)
+ Poisson counting noise
+ Neutron background
  (only direct so far)

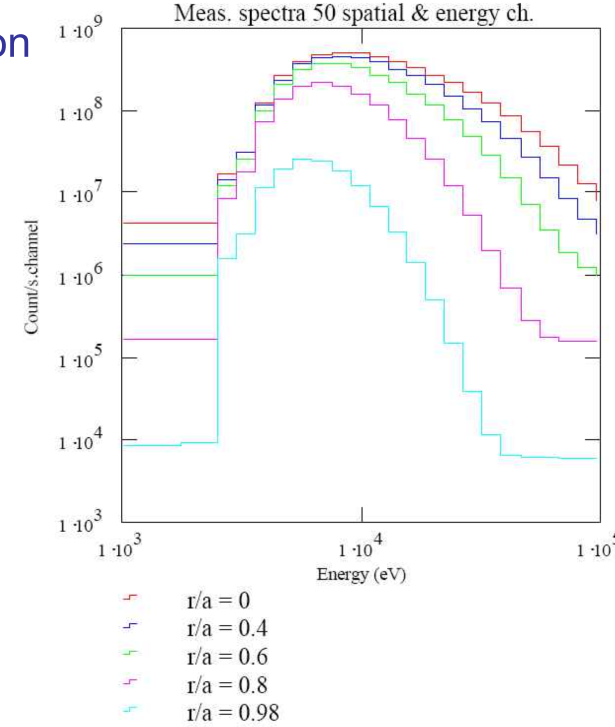

Analytic Abel inversion

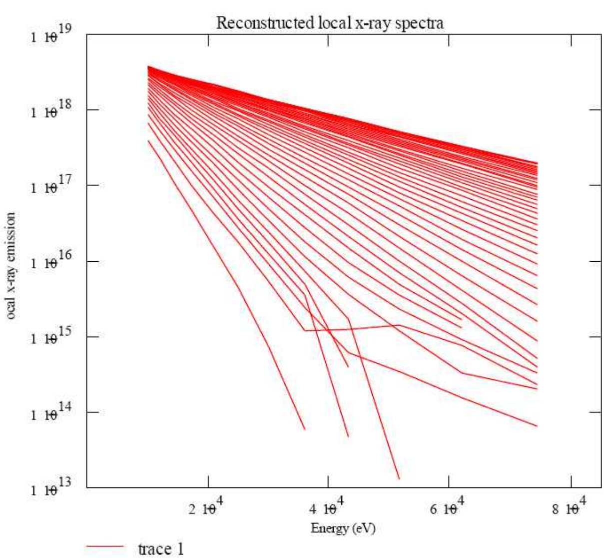

Fit 1/e gradient for local Te at each chord

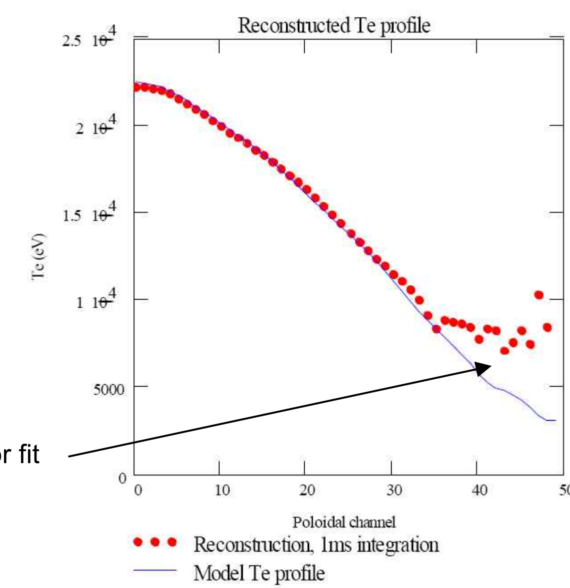

Artefact due to fixed energy range for fit at each chord. Can be improved

Radial and vertical x-ray cameras in Eq09 and Up09

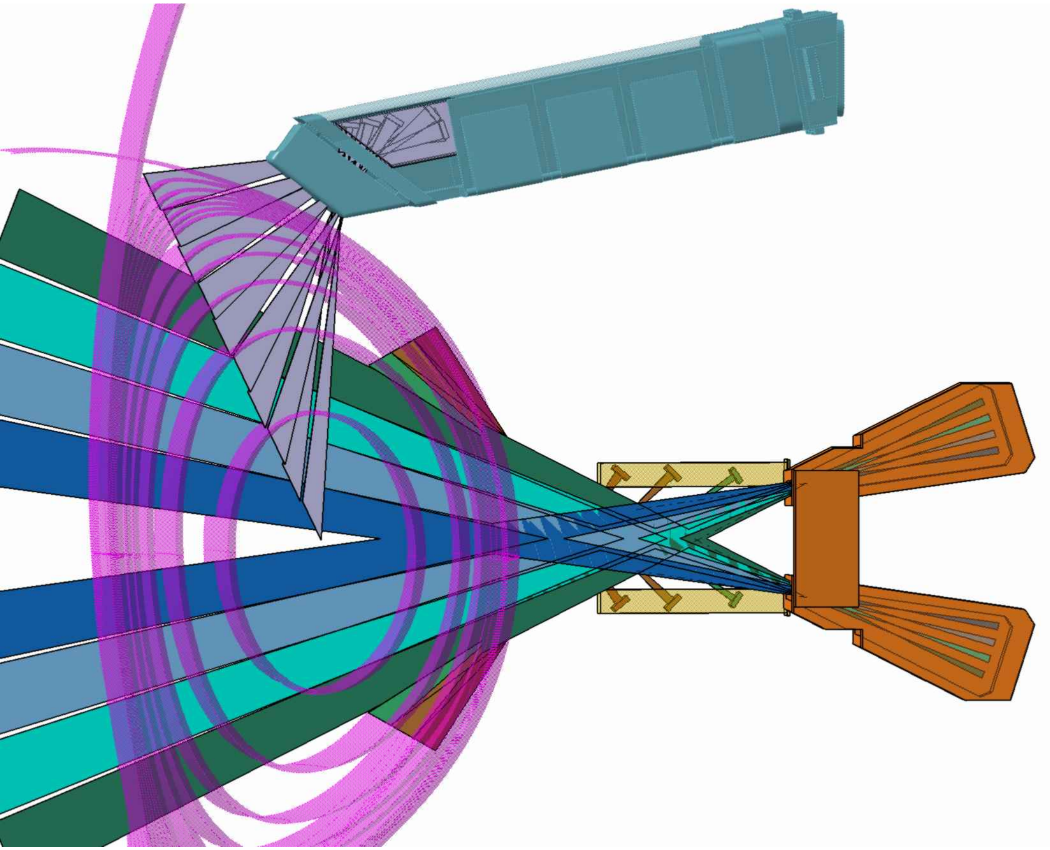

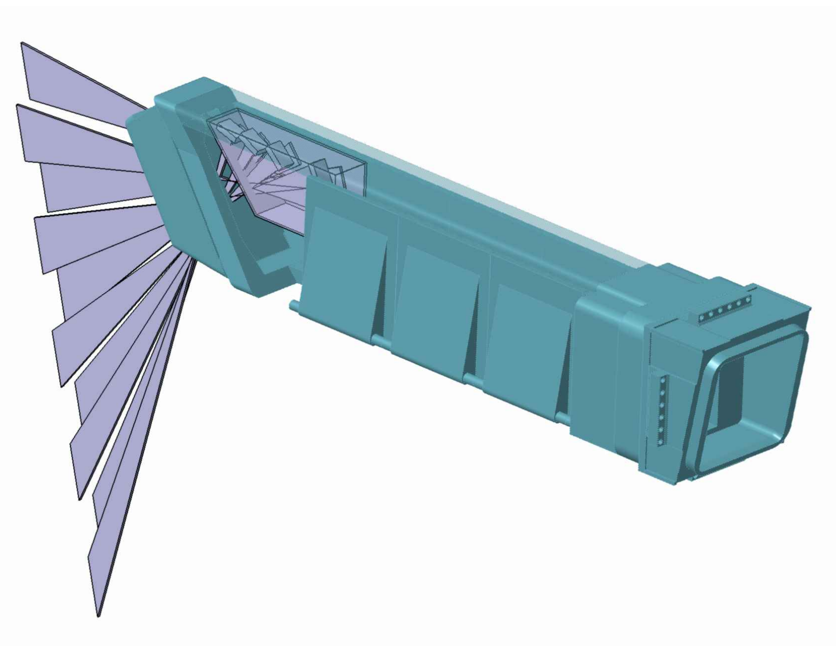

1mm spatial resolution possible with 100 um slit

Detectors outside port or in removable cassettes

Radial camera:	Full poloidal coverage	Edge views most vulnerable
Vertical camera:	Coverage inboard of rho=0	Core views most vulnerable

Summary

- **X-ray camera is uncredited, though design and R+D is progressing**

- **Both Physics and Technology for x-rays get better at higher energy**
- High quality, low-risk measurement
- Potential to measure the detailed electron energy spectrum

- **New generation of detectors make fast, imaging x-ray PHA possible**
- Spatial resolution 1-10 mm – 100 -1000 chords for good tomography
- Time resolution ~ 1ms (current mode even faster)
- Energy resolution 5 – 15%

- **Integrated into ITER equatorial port 09 and upper port 09**
- Similar to Radial Neutron Camera, but smaller apertures
- Robust windows for > 10 keV
- Detectors in removable cassettes